Subclinical cartilage degeneration in young athletes with posterior cruciate ligament injuries detected with T1ρ magnetic resonance imaging mapping.	Okazaki K, Takayama Y, Osaki K, Matsuo Y, Mizu-Uchi H, Hamai S, Honda H, Iwamoto Y	*Knee Surg Sports Traumatol Arthrosc*	2014 Dec (E-pub)	国外
CCAAT/enhancer-binding protein β promotes receptor activator of nuclear factor-kappa-B ligand (RANKL) expression and osteoclast formation in the synovium in rheumatoid arthritis	Tsushima H, Okazaki K, Ishihara K, Ushijima T, Iwamoto Y	*Arthritis Research & Therapy*	2015 Feb, 17(1):532	国外

Ishihara et al. Journal of Orthopaedic Surgery and Research 2014, 9:98
http://www.josr-online.com/content/9/1/98

JOURNAL OF ORTHOPAEDIC SURGERY AND RESEARCH

RESEARCH ARTICLE Open Access

Simultaneous regeneration of full-thickness cartilage and subchondral bone defects *in vivo* using a three-dimensional scaffold-free autologous construct derived from high-density bone marrow-derived mesenchymal stem cells

Kohei Ishihara[1], Koichi Nakayama[1,2*], Shizuka Akieda[1], Shuichi Matsuda[1] and Yukihide Iwamoto[1]

Abstract

Background: In recent years, several methods have been developed for repairing full-thickness cartilage defects by tissue engineering using mesenchymal stem cells. Most of these use scaffolds to achieve sufficient thickness. However, considering the potential influence of scaffolds on the surrounding microenvironment, as well as immunological issues, it is desirable to develop a scaffold-free technique. In this study, we developed a novel technique, a scaffold-free autologous construct derived from bone marrow-derived mesenchymal stem cells (BM-MSCs), and successfully use this technique to regenerate cartilage and subchondral bone to repair an osteochondral defect in rabbit knees.

Methods: BM-MSCs were isolated from bone marrow liquid aspirated from the iliac crest of rabbits. After expansion in culture dishes and re-suspension in 96-well plates, the cells spontaneously aggregated into a spheroid-like structure. The spheroids were loaded into a tube-shaped Teflon mold with a 5-mm height and maintained under air-liquid interface conditions. These loaded spheroids fused with each other, resulting in a cylinder-shaped construct made of fused cells that conformed to the inner shape of the mold. The construct was implanted into an osteochondral defect in rabbit knees and histologically analyzed 24 and 52 weeks after implantation using Wakitani's scoring system.

Results: Both bone and cartilage were regenerated, maintaining a constant thickness of cartilage. The mean histological score was 10 ± 1.7 in the 24-week group and 9.7 ± 0.6 in the 52-week group. There was no significant difference between the 24- and 52-week groups in either parameter of the score, indicating that no deterioration of the repaired tissue occurred during the intervening period.

Conclusions: Using our novel technique, which employs a three-dimensional scaffold-free autologous construct derived from BM-MSCs, we successfully achieved simultaneous regeneration of bone and cartilage for up to 1 year *in vivo*. This method has potential for clinical use as a safe and effective method for repairing bone and cartilage defects.

Keywords: Tissue engineering, Mesenchymal stem cells, Osteochondral cartilage defect, Scaffold-free, Cartilage repair

* Correspondence: nakayama@me.saga-u.ac.jp
[1]Department of Orthopaedic Surgery, Graduate School of Medical Sciences, Kyushu University, 3-1-1 Maidashi, Higashi-ku, Fukuoka City, Fukuoka 812-8582, Japan
[2]Department of Advanced Technology Fusion, Graduate School of Science and Engineering, Saga University, 1 Honjo-machi, Saga City, Saga 840-8502, Japan

Background

Repairing damaged cartilage, as in traumatic lesions of the joint surface or degenerative damage due to osteoarthritis, remains a clinical challenge because of the poor self-healing ability of cartilage [1]. Several existing treatments for the repair of damaged cartilage, including mosaicplasty [2], microfracture [3], and autologous chondrocyte implantation (ACI) [4], have been used successfully in patients to relieve pain and improve joint function. However, the long-term results of mosaicplasty and microfracture are unsatisfactory because the replaced tissue is not physiological hyaline cartilage, but mostly fibrous cartilage, which lacks suitable mechanical properties [5,6]. Furthermore, in histological evaluations of the repaired tissue, ACI exhibited no significant difference compared to microfracture in a randomized trial [7], and the repaired tissue was predominantly fibrous cartilage.

Tissue engineering of functional articular cartilage could help address these issues. In recent years, several methods have been developed to repair full-thickness cartilage defects. Some of these methods use synthetic or biological scaffolds to achieve sufficient thickness, mechanical function, support cell attachment, migration, proliferation, and differentiation [8,9]. However, these materials can influence the surrounding microenvironments [10] or cause immunological problems [11,12].

Several scaffold-free systems have also been investigated [13-16]. Without using a scaffold, however, it is difficult to create enough thickness to fill in the defect. A thickness of 5 mm is necessary to fill a full-thickness articular cartilage defect in the knee. Furthermore, with or without using a scaffold, it is even more challenging for the current methods to regenerate both articular cartilage and subchondral bone in the context of an osteochondral defect, which sometimes occurs in trauma, osteochondritis dissecans, osteonecrosis, or osteoarthritis.

Adherent cells grown in suspension form spheroids (aggregates) in order to avoid cell death. We confirmed this phenomenon using bone marrow-derived mesenchymal stem cells (BM-MSCs). Furthermore, we developed a novel method for fusing spheroids derived from BM-MSCs to make a large construct without using a scaffold. Loading the spheroids into a molding chamber can produce a columnar structure consisting of fused spheroids; we named this structure "high-density mesenchymal stem cell, scaffold-free autologous construct" (HDMAC). We hypothesized that HDMACs could be used to regenerate both articular cartilage and subchondral bone in the context of an osteochondral defect. Furthermore, because many other reports have achieved successful short-term cartilage repair, we focused on achieving a relatively long-term result (up to 1 year) in an animal model.

The purposes of this study were to demonstrate our method for making spheroids and a scaffold-free construct (HDMAC) using only undifferentiated BM-MSCs and to evaluate the 1-year outcome of simultaneous regeneration of cartilage and subchondral bone in an osteochondral defect in rabbit knees.

Materials and methods

Rabbits

All experiments followed protocols approved by the institutional animal care and use committee (approval number: A21-204-2). Fifteen mature female Japanese white rabbits (Japan Kyudo Inc, Tosu, Japan) with a mean weight of 3.9 kg (range 3.5–4.2) were eventually used for this study after several pilot studies to establish the procedures in detail. Animals were housed in separate cages at the animal center of our institution with free access to water and standard food. Two or three rabbits were euthanized at 3, 6, and 12 weeks and three rabbits were euthanized at each of two time points (24 and 52 weeks) after implantation for histological analysis.

Culture medium

Dulbecco's modified Eagle's medium (DMEM) (Nissui #05915, Nissui Pharmaceutical, Tokyo, Japan) containing 10% fetal bovine serum (FBS) (HyClone, Logan, UT, USA), 100 U/mL penicillin, and 100 μg/mL streptomycin (Sigma-Aldrich, St. Louis, MO, USA) was used. No differentiation agents were used from cell isolation to construct formation.

Isolation and culture of mesenchymal stem cells (MSCs)

MSCs were isolated as described previously with some modifications in the method [9]. Briefly, bone marrow liquid was aspirated from the iliac crest of the rabbits under general anesthesia, and the obtained bone marrow was mixed with heparin. After centrifugation at 1,000 rpm for 5 min, the buffy coat of the bone marrow liquid was aspirated and expanded into a 15-cm culture dish containing DMEM and 10% FBS. The cells obtained were expanded until they reached the necessary numbers ($\sim 4 \times 10^7$ cells).

Spheroid formation

Cells were detached by recombinant trypsin replacement, re-suspended in DMEM plus 10% FBS, and then divided into 96-well plates designed to prevent cells from adhering to the culture surface (Sumilon PrimeSurface, Sumitomo Bakelite, Tokyo, Japan) at 4×10^4 cells per well. After incubation at 37°C and 5% CO_2 for 2 days, the cells spontaneously aggregated into a spheroid-like structure (Figure 1a).

Construct formation

The spheroids described above were loaded into a handmade tube-shaped Teflon mold with a diameter of 4.6 mm and a height of 5 mm (Figure 1b). At the bottom

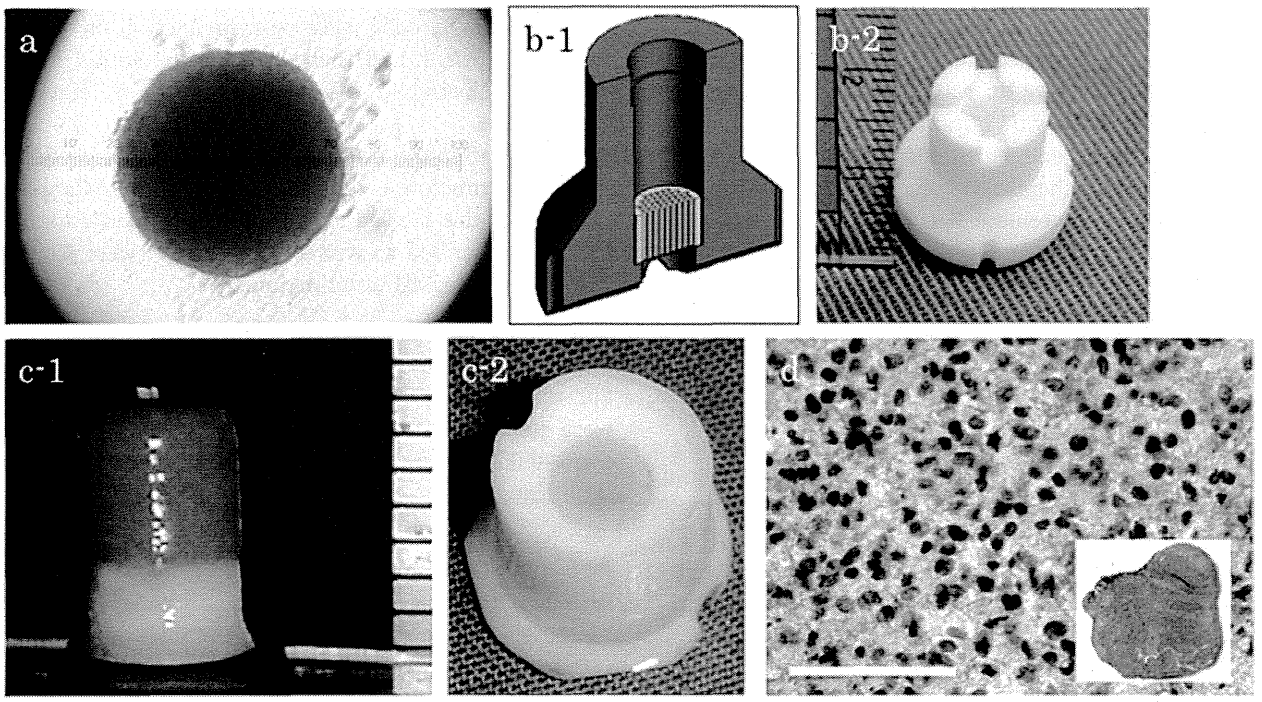

Figure 1 Manufacturing HDMACs. (a) BM-MSCs were isolated from bone marrow liquid aspirated from rabbits. After expansion, re-suspension, and incubation, the cells spontaneously aggregated into a spheroid-like structure. Each scale unit represents 1 μm. **(b)** A handmade tube-shaped Teflon mold with a diameter of 4.6 mm and a height of 5 mm. The spheroids described in **(a)** were loaded into this mold. Each scale unit represents 1 mm. **(c)** The tube-shaped mold was maintained under air-liquid interface conditions and incubated for a week. These loaded spheroids fused with each other, and a cylinder-shaped construct made with fused cells was obtained according to the inner shape of the mold. Each scale unit represents 1 mm. **(d)** Safranin O staining of HDMACs after 1 week of incubation. Scale bar =100 μm. ($N = 1$).

of the mold, a base disc was placed into the chamber; the base disc was used for handling of the construct. Six hundred to seven hundred spheroids were needed to make one construct. The tube-shaped mold was maintained under air-liquid interface conditions and incubated at 37°C and 5% CO_2 for 1 week in DMEM plus 10% FBS.

These loaded spheroids fused with each other, resulting in formation of a cylinder-shaped construct made of fused cells that conformed to the inner shape of the mold (Figure 1c). We named these structures "high-density mesenchymal stem cell, scaffold-free autologous constructs" (HDMACs).

Scanning electron microscopy (SEM)

Constructs were fixed with 1% glutaraldehyde/1.44% paraformaldehyde in buffer at 37°C for 60 min, frozen in liquid nitrogen, and lyophilized. Next, samples were sputter-coated with an alloy of platinum and palladium and then observed by scanning electron microscopy (JSM 840A, JEOL USA, Peabody, MA, USA).

Implantation *in vivo*

After general anesthesia, a cylindrical defect was created in the articular cartilage of the patella groove. The diameter of the defect was set to 4.8 mm. The depth was determined to be the same as the height of the cell construct, usually 4–5 mm in depth, which reached the middle layer of the subchondral bone. The construct was gently implanted into the defect, the Teflon disc was removed, and the top of the construct was flattened using the surgeon's finger. No patches were placed on the implant surface. The osteochondral defect in the contralateral knee was left empty for controls. After washing and closure of the wound, the knee was immobilized with a cast for 1 week. In a pilot study, individual rabbits were euthanized at 3, 6, and 12 weeks to confirm the early regeneration process by histological evaluation. After obtaining positive results from this pilot study, three knees were obtained at each of two time points (24 and 52 weeks) and subjected to histological analysis.

Micro-CT scanning

For morphological observation, the specimens were scanned using a micro-CT (Hitachi-Aloka Medical, Tokyo, Japan) after euthanasia. Sliced CT data were three-dimensionally reconstructed (Real INTAGE, Kubota Graphics Technology, Tokyo, Japan).

Histological analysis and immunohistochemistry

Specimens were fixed in 4% paraformaldehyde, decalcified with 0.5 M ethylenediaminetetraacetic acid (EDTA), and embedded in paraffin wax. Sagittal sections (5 μm thick) were stained with safranin O and Weigert's iron hematoxylin and then examined by light microscopy. For immunohistochemistry, sections were pretreated with 0.4 mg/mL proteinase K (DAKO, Carpinteria, CA, USA) for 10 min at room temperature. Endogenous peroxidases were quenched using 3% hydrogen peroxide in methanol for 20 min at room temperature. The sections were then incubated with mouse polyclonal antibody against type II collagen (F-57 anti-hCL (II), FUJI Chemical Industries, Toyama, Japan) and rabbit polyclonal antibody against type X collagen (ab58632, Abcam, Cambridge, MA, USA) at room temperature for 1 h. The immunostaining was performed using the VECTASTAIN ABC reagent (Vector Laboratories, Burlingame, CA, USA) and developed in 3,3'-diaminobenzidine and 0.02% H_2O_2 with hematoxylin counterstaining.

Histological scoring

Histological findings were scored according to a scale described by Wakitani et al. [9]. Sections were graded according to 1) cell morphology (maximum 4 points), 2) matrix staining (maximum 3 points), 3) surface regularity (maximum 3 points), 4) thickness of cartilage (maximum 2 points), and 5) integration of donor material into adjacent host cartilage (maximum 2 points). Scoring was performed blindly by two orthopedic surgeons who were independent of this study, and the average of each score was adopted.

Cell tracking

At first passage, cells were re-suspended at in DMEM 1.0×10^6 cells/mL and then were labeled with Qtracker 655 Cell Labeling Kit (Quantum Dot Corp., Hayward, CA, USA).

The day after the cell labeling, the cells proceeded to spheroid formation as described above. HDMACs generated using the labeled cells were implanted in rabbit knees as described above, and the rabbits were 6 weeks later for histological examination.

Statistical analysis

For *in vivo* investigations, nonparametric comparisons were performed using Student's *t* test. *P* values less than 0.05 were considered to represent statistical significance.

Results

Histology and scanning electron micrographs of HDMACs

Histological examination of HDMACs with safranin O staining after 1 week of incubation revealed that the nucleus of cells were stained without fragmentation or chromatin condensation at the whole area of the section, suggesting that the cells in the construct were viable and did not undergo apoptosis (Figure 1d). The matrix was not stained red, suggesting that the cells in the HDMACs had not been differentiated into chondrocytes before the implantation. The ultrastructural morphology of the HDMACs was assessed by SEM. The micrographs revealed that these constructs contained flattened cells with some amount of collagen fibers (Figure 2).

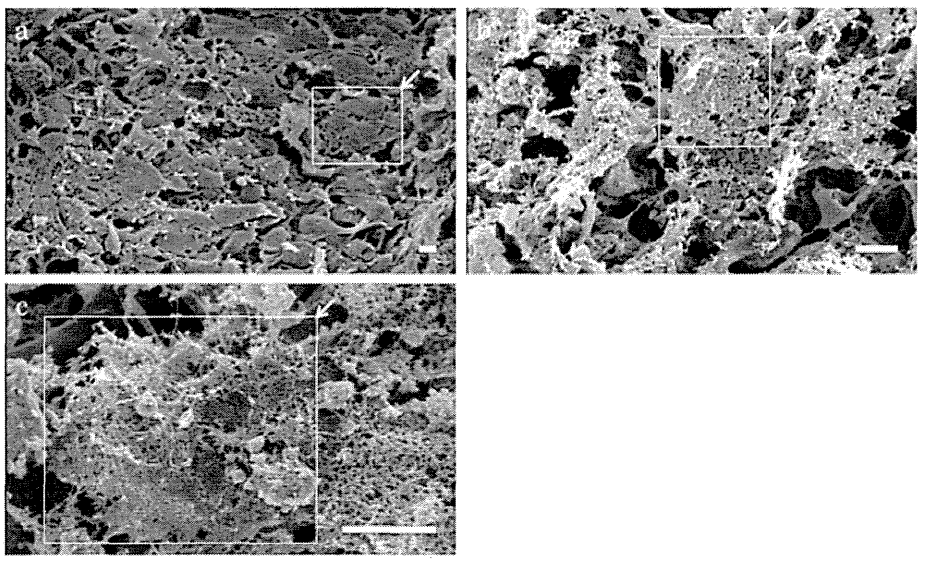

Figure 2 Scanning electron micrographs of HDMACs. SEMs showed that these constructs contained flattened cells (arrows and frames) with some amount of collagen fibers. Original magnifications were **(a)** 430×, **(b)** 1,000×, and **(c)** 2,500×. Scale bar =10 μm. (*N* = 1).

Pilot study for early repairing process in osteochondral defect

To test our hypothesis that HDMACs would be able to simultaneously regenerate cartilage and bone, two or three rabbits were euthanized at 3, 6, and 12 weeks and morphologically and histologically assessed (Figures 3a–i and 4a–i). After 6 weeks of implantation, the surface of the defect was covered with cartilaginous white tissue. Micro-CT scanning also suggested that bone formations were present at the peripheral areas and developed toward the central area. Histological examination suggested that cartilaginous differentiation, which was detected by safranin O staining and immunostaining for type II collagens, occurred at peripheral areas of the implanted HDMACs and developed toward the central area. At 6 weeks, all the implanted area showed positive staining for safranin O and type II collagen. At 12 weeks, endochondral bone formation progressed, and almost the whole area corresponding to the subchondral bone was replaced by bone structures. At the joint surface area of the implanted tissue, hyaline cartilage was regenerated with a constant thickness.

By contrast, in a control rabbit without any implantation, the defect was filled with fibrous tissue. Although a spontaneous repairing process was observed at the peripheral area that showed slight staining for safranin O or type II collagen, the cartilage formation and the subchondral bone formation were incomplete at the central area even at 12 weeks (Figures 3j–l and 4j–l).

Cell tracking

HDMACs were made with labeled MSCs and implanted into the osteochondral defect. Labeled cells were detected as chondrocytes in the cartilage and osteocytes in the subchondral bone 6 weeks after implantation, suggesting that the implanted MSCs had spontaneously differentiated into chondrocytes or osteocytes in accordance with their implanted positions (Figure 5).

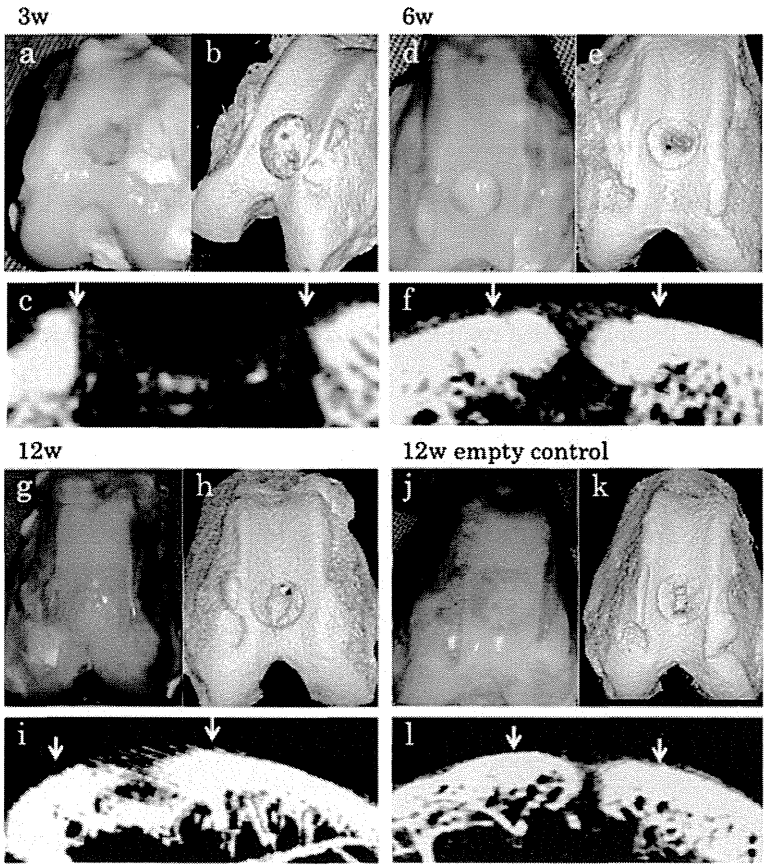

Figure 3 Early repair processes in osteochondral defects. Gross appearance at **(a)** 3 weeks, **(d)** 6 weeks, and **(g)** 12 weeks. After 6 weeks of implantation, the surface of the defect was covered with cartilaginous white tissue. Micro-CT scanning at **(b, c)** 3 weeks, **(e, f)** 6 weeks, and **(h, i)** 12 weeks suggested that bone formations were present at the peripheral areas and developed toward the central area. **(j)** Gross appearance and **(k, l)** micro-CT scanning of a control rabbit without any implantation at 12 weeks. Although the gross appearance showed that the defect was filled with white tissues, the subchondral bone formation was incomplete at the center of the defect at 12 weeks. Downwards arrows indicate the borders of the defect. Representative subjects of two or three experiments for each time course are shown.

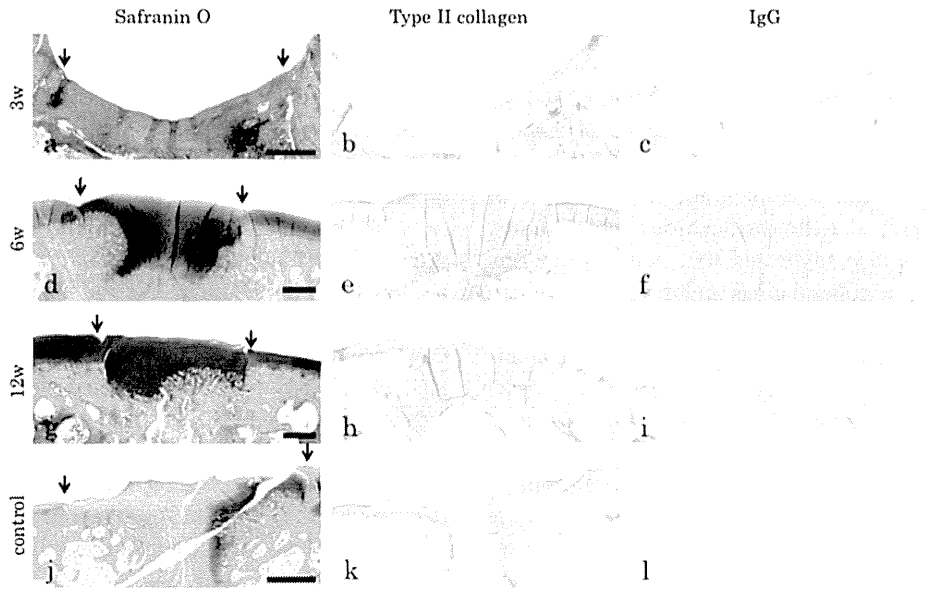

Figure 4 Histological examination at early repair processes in osteochondral defects. Safranin O staining, immunostaining for type II collagens, and IgG staining as controls at **(a–c)** 3 weeks, **(d–f)** 6 weeks, and **(g–i)** 12 weeks after the implantation. At 3 weeks, the implanted tissue had not differentiated into hyaline cartilage yet. At 6 and 12 weeks, the joint surface area of the implanted tissue was stained with safranin O and immunostained for type II collagen. Endochondral bone formation was observed at the peripheral area at 6 weeks and developed toward the central area at 12 weeks. **(j–l)** A control rabbit without any implantation at 12 weeks. The defect was filled with fibrous tissue that did show a constant staining for safranin O and immunostaining for type II collagen, especially at the surface and central areas. Scale bar = 1 mm. Downwards arrows indicate the borders of the defect. Representative subjects of two or three experiments for each time course are shown.

Histological examination at 24 and 52 weeks

After obtaining the preliminary results regarding the early regeneration process, we focused on morphological and histological evaluation at 24 and 52 weeks (n = 3 each) (Figures 6a–j and 7a–h). CT scans revealed complete regeneration of the subchondral bone. Histological examination revealed that hyaline cartilage, which was stained for safranin O and immunostained for type II collagen, was maintained at a consistent thickness identical to that of the surrounding original cartilage at both 24 and 52 weeks.

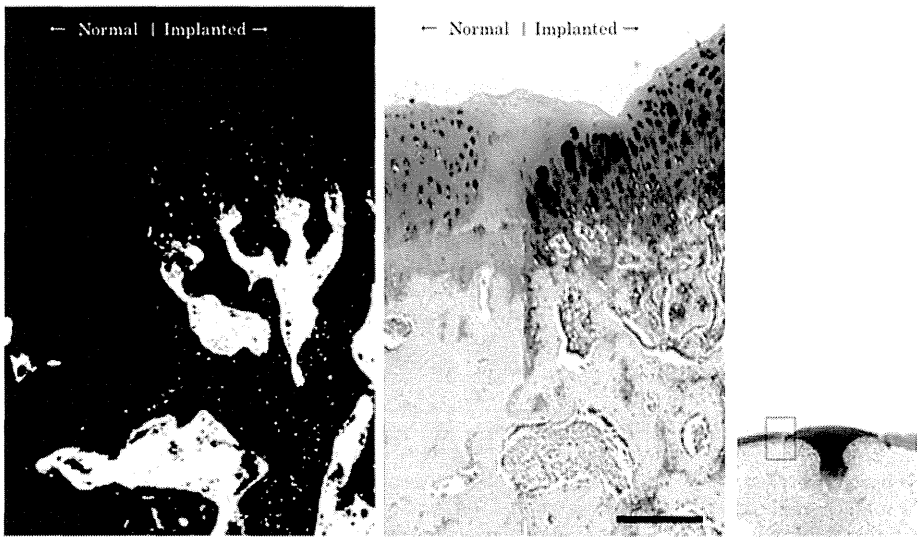

Figure 5 Cell tracking. HDMACs made with labeled MSCs were implanted to the osteochondral defect. The labeled cells were detected as chondrocytes in the cartilage and osteocytes in the subchondral bone 6 weeks after implantation, suggesting that the implanted MSCs had spontaneously differentiated into chondrocytes or osteocytes in accordance with their implanted positions. Scale bar = 200 μm. (N = 1).

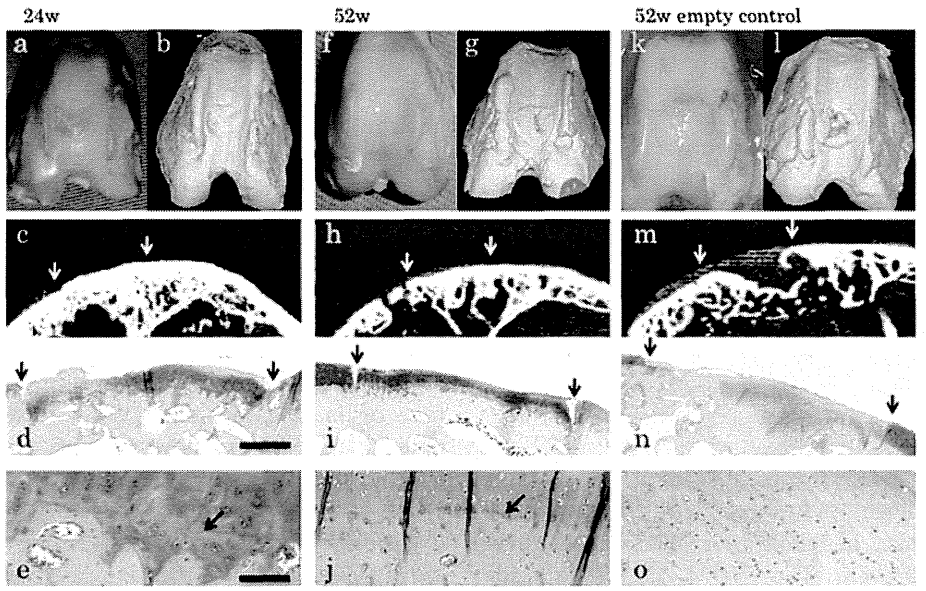

Figure 6 Morphological and histological examination at 24 and 52 weeks. Gross appearance, micro-CT scanning, and safranin O staining at **(a–e)** 24 weeks and **(f–j)** 52 weeks. Micro-CT scans revealed complete regeneration of the subchondral bone. Histological examination revealed that the regenerated cartilage was maintained with a consistent thickness identical to that of the surrounding original cartilage at both **(d)** 24 weeks and **(i)** 52 weeks. Scale bar = 1 mm. **(e, j)** Tidemarks, which separate hyaline cartilage from the calcified cartilage, were seen (arrows). Scale bar = 100 μm. **(k–o)** A control rabbit without any implantation at 52 weeks. The defect was mainly filled with fibrous tissue that did not exhibit formation of subchondral bone **(m)** or sufficient staining with safranin O **(n)**. Although some area was stained with safranin O, tidemark was not formed **(o)**. Downwards arrows indicate the borders of the defect. Representative subjects of three experiments for each time course are shown.

Immunostaining for type X collagens did not show positive staining in the implanted area during the regeneration period. Tidemark, which separates hyaline cartilage from the calcified cartilage layer, was seen in these two groups, suggesting the integrality of the regenerated articular structures. By contrast, a control rabbit without any implantation showed that the defect was mainly filled with fibrous tissue that did not exhibit the consistent staining for safranin O or formation of the subchondral bone. Although some area was stained with safranin O, tidemark was not formed (Figure 6k–o).

The mean histological score was 10 ± 1.7 (standard error (S.E.)) in the 24-week group and 9.7 ± 0.6 (S.E.) in the 52-week group. There was no significant difference between the 24- and 52-week groups in either parameter of the score, indicating that no deterioration of the repaired tissue took place during this period (Table 1).

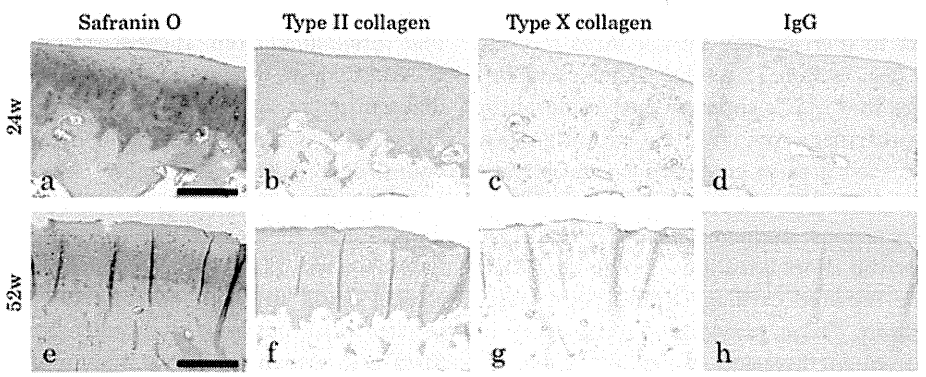

Figure 7 Immunohistochemistry at 24 and 52 weeks. Safranin O staining **(a, e)**, immunostaining for type II collagens **(b, f)**, immunostaining for type X collagens **(c, g)**, and IgG staining as controls **(d, h)** at 24 weeks **(a–d)** and 52 weeks **(e–h)**. No positive Immunostaining for type X collagens was observed in the implanted area during the regeneration period. Scale bar =200 μm. Representative subjects of three experiments for each time course are shown.

Table 1 Histological scores at 24 and 52 weeks after implantation

	24 weeks (n =3)	52 weeks (n =3)	p value
Cell morphology	2.7 (2–3)	2.7 (2–3)	N.S.
Matrix staining (metachromasia)	1.7 (1–2)	1.7 (1–2)	N.S.
Surface regularity	3	3	N.S.
Thickness of cartilage	1.3 (1–2)	1.7 (1–2)	N.S.
Integration of donor to adjacent host cartilage	1.3 (1–2)	0.7 (0–1)	N.S.
Total score (score range 0–14)	10 (8–11)	9.7 (9–10)	N.S.

N.S. not significant.

Discussion

In this study, we demonstrated successful regeneration of articular cartilage and subchondral bone in an osteochondral defect of rabbit knee joints using three-dimensional HDMACs. The HDMACs were made without using any differentiation agents, such as growth factors, and were implanted to the osteochondral defect while the cells in the construct were undifferentiated. The implanted MSCs spontaneously differentiated into bone or cartilage, depending on the environment in which they were implanted, and maintained the original border between bone and cartilage. Eventually, by the 52-week follow-up, the simultaneous regeneration of bone and cartilage had been completed. The unique features of our method are as follows: 1) A three-dimensional MSC construct with sufficient thickness for bone and cartilage repair can be made without a scaffold. 2) The construct is implanted without induction of differentiation. 3) Simultaneous regeneration of bone and cartilage occurs spontaneously by reproducing the differentiation process involved in bone and cartilage formation. A major strength of our study is that we could confirm that the regenerated bone and cartilage were maintained for up to 52 weeks.

However, one limitation of our study is that we did not make an effort to increase the sample sizes for the short-term results (e.g., within 12 weeks). After confirming in a few samples that MSCs spontaneously differentiate into bone or cartilage *in vivo*, as we originally hypothesized, we placed greater emphasis on investigating the long-term results. We chose this course because a large number of previous studies using other methods had succeeded over the short term, but it remained that deterioration of the repaired cartilage would occur over long-term observation. Some previous studies using a scaffold reported frequent invasion of a bony structure into the repaired cartilage, causing the cartilage to become thinner than the surrounding normal articular cartilage [9,17]. Furthermore, a scaffold has the potential to influence surrounding microenvironments, which can affect the regional specification of implanted MSCs [10]. The presence of nonphysiological scaffolds could interfere with the physiological distribution of signal molecules, such as growth factors, that influence the differentiation of cells toward bone and cartilage.

Following a report of the efficacy of ACI by Brittberg et al. [4], chondrocytes have been widely used in the field of articular cartilage regeneration. The form of the grafts used for implantation varies from monolayer culture [4] to tissue-engineered three-dimensional cultures in agarose [18] or atelocollagen gel [19]. A number of clinical trials have been conducted, and some of them reported successful outcomes in regard to patients' symptoms or imaging endpoints [19,20]. However, it should be noted that ACI was more effective in patients younger than 45 years than in older patients [21]. In fact, the mean age of clinical trials with satisfactory outcomes for relatively long follow-up periods ranges from 26.4 to 33.1 years old [19,22]. This result may be related to the shortening of telomeres in many adult cells, including chondrocytes [23]. Therefore, it may be necessary to use alternative methods in middle-aged and elderly patients.

Bone and cartilage have the same origin, i.e., MSCs. In a previous work, patient age made no difference in outcomes of methods using MSCs [21]. Therefore, MSCs represent an attractive alternative to adult chondrocytes as a cell source for bone and cartilage regeneration. However, it is challenging to artificially control differentiation into the osteocyte or chondrocyte lineage after implantation. The underlying molecular mechanism of our method, in which a bone and articular cartilage defect was repaired while maintaining the border between cartilage and subchondral bone, is currently unclear. However, cell tracking analysis revealed that both cell types in the repaired tissues were derived dominantly from the implanted MSCs within the construct rather than the migrated cells from the surrounding tissues (Figure 5). Our HDMACs may mimic the cellular integration of embryonic osteogenesis and chondrogenesis that originates from mesenchymal condensation. The HDMACs were implanted without pretreatment to induce differentiation. The micrographs by SEM revealed that the HDMACs contained flattened cells, not ovary-shaped chondrocyte-like cells (Figure 2). Combined with the fact that the HDMACs were not stained with safranin O (Figure 1d), these cells are suggested to be undifferentiated. On the other hand, we also confirmed that the constructs could undergo differentiation into chondrocytes *in vitro* when cultured in chondrocyte induction medium (data not shown). *In vivo*, the implanted MSCs spontaneously differentiate into articular cartilage and subchondral bone; eventually, the normal structures of bone and cartilage were completely formed (Figures 6 and 7). In addition, type X collagen was not expressed in the

implanted area. This suggests that hypertrophy of articular cartilage, one of the major problems using MSC-based constructs, did not occur during the regeneration period.

Our study is distinguished not only by the use of undifferentiated MSCs but also by the use of a construct generated by a scaffold-free method. Our HDMACs have enough volume to fill a full-thickness cartilage defect. Cell nutrition particularly in the middle of a big construct can be a concern [24]. However, the nucleus was stained with hematoxylin in the middle of the HDMACs and there was no fragmentation or chromatin condensation (Figure 1d). This suggests that the cells in the construct were viable. Previous studies developed various scaffold-free methods using chondrocytes or MSCs; the simplest reported method is injection of synovial MSCs into a cartilage defect *in vivo* [16]. In that study, however, although the histological score was significantly greater than the control, the depth of the defect was restricted to 2 mm and the surface was concave. Another method using a scaffold-free construct derived from synovial MSCs resulted in successful repair of a cartilage defect [14], but again, the depth was limited to 2 mm. In yet another study, scaffold-free chondrocyte sheets were used successfully to repair of a partial-thickness cartilage defect *in vivo* [13]. However, this method was insufficient for subchondral bone repair and tissue integration in the context of a full-thickness cartilage defect [25]. In efforts to obtain enough cell mass to fill a full-thickness cartilage defect, pellet cultures of chondrocytes or MSCs have been investigated. In one animal study, chondrocyte pellet implantation into a 3-mm osteochondral defect was attempted [15]. Although the thickness of the repaired cartilage remained relatively constant, overgrowth of the surface was observed, and subchondral bone regeneration was extremely limited.

Conclusions

Our novel technique, using a three-dimensional scaffold-free autologous construct derived from BM-MSCs, successfully achieved the simultaneous regeneration of bone and cartilage for up to 1 year *in vivo*. This method has potential for clinical use as a safe and effective method for repairing bone and cartilage defects.

Competing interests

KN is a co-founder and a shareholder of Cyfuse Biomedical K.K., Tokyo, Japan. The other authors declare that they have no competing interests.

Authors' contributions

KN designed the study and executed the experimental setup. KI participated in the data analysis and drafted the manuscript. SA participated in the execution of the experiment and discussion. SM and YI provided important feedback on the experimental setup and participated in the discussion. All authors read and approved the final version of the manuscript.

Acknowledgements

The authors thank Dr. Ken Okazaki, Department of Orthopaedic Surgery at Kyushu University Hospital, for the support in preparing the manuscript and Dr. Takaaki Kanemaru, Morphology Core Unit at Kyushu University, for kindly observing the HDMACs by SEM. This study was partially supported by JST Translational Research Network Program No. 08061012.

Received: 27 June 2014 Accepted: 7 October 2014
Published online: 14 October 2014

References

1. Buckwalter JA, Mankin HJ: **Articular cartilage repair and transplantation.** *Arthritis Rheum* 1998, **41**:1331–1342.
2. Matsusue Y, Yamamuro T, Hama H: **Arthroscopic multiple osteochondral transplantation to the chondral defect in the knee associated with anterior cruciate ligament disruption.** *Arthroscopy* 1993, **9**:318–321.
3. Steadman JR, Briggs KK, Rodrigo JJ: **Outcomes of microfracture for traumatic chondral defects of the knee: average 11-year follow-up.** *Arthroscopy* 2003, **19**:477–484.
4. Brittberg M, Lindahl A, Nilsson A: **Treatment of deep cartilage defects in the knee with autologous chondrocyte transplantation.** *N Engl J Med* 1994, **331**:889–895.
5. Kreuz P, Steinwachs M, Erggelet C, Krause S, Konrad G, Uhl M, Sudkamp N: **Results after microfracture of full-thickness chondral defects in different compartments in the knee.** *Osteoarthritis Cartilage* 2006, **14**:1119–1125.
6. Bentley G, Biant LC, Carrington RWJ, Akmal M, Goldberg A, Williams AM, Skinner JA, Pringle J: **A prospective, randomised comparison of autologous chondrocyte implantation versus mosaicplasty for osteochondral defects in the knee.** *J Bone Joint Surg (Br)* 2003, **85-B**:223–230.
7. Knutsen G, Engebretsen L, Ludvigsen TC, Drogset JO, Grøntvedt T, Solheim E, Strand T, Roberts S, Isaksen V, Johansen O: **Autologous chondrocyte implantation compared with microfracture in the knee. A randomized trial.** *J Bone Joint Surg Am* 2004, **86**:455–464.
8. Wakitani S, Kimura T, Hirooka A, Ochi T, Yoneda M, Yasui N, Owaki H, Ono K: **Repair of rabbit articular surfaces with allograft chondrocytes embedded in collagen gel.** *J Bone Joint Surg (Br)* 1989, **71**:74–80.
9. Wakitani S, Goto T, Pineda SJ, Young RG, Mansour JM, Caplan AI, Goldberg VM: **Mesenchymal cell-based repair of large, full-thickness defects of articular cartilage.** *J Bone Joint Surg Am* 1994, **76**:579–592.
10. Koga H, Muneta T, Ju YJ, Nagase T, Nimura A, Mochizuki T, Ichinose S, Mark von der K, Sekiya I: **Synovial stem cells are regionally specified according to local microenvironments after implantation for cartilage regeneration.** *Stem Cells* 2007, **25**:689–696.
11. Anderson JM, Rodriguez A, Chang DT: **Foreign body reaction to biomaterials.** *Semin Immunol* 2008, **20**:86–100.
12. Badylak SF, Gilbert TW: **Immune response to biologic scaffold materials.** *Semin Immunol* 2008, **20**:109–116.
13. Kaneshiro N, Sato M, Ishihara M, Mitani G, Sakai H, Mochida J: **Bioengineered chondrocyte sheets may be potentially useful for the treatment of partial thickness defects of articular cartilage.** *Biochem Biophys Res Commun* 2006, **349**:723–731.
14. Ando W, Tateishi K, Hart DA, Katakai D, Tanaka Y, Nakata K, Hashimoto J, Fujie H, Shino K, Yoshikawa H, Nakamura N: **Cartilage repair using an in vitro generated scaffold-free tissue-engineered construct derived from porcine synovial mesenchymal stem cells.** *Biomaterials* 2007, **28**:5462–5470.
15. Cheuk Y-C, Wong MW-N, Lee K-M, Fu S-C: **Use of allogeneic scaffold-free chondrocyte pellet in repair of osteochondral defect in a rabbit model.** *J Orthop Res* 2011, **29**:1343–1350.
16. Nakamura T, Sekiya I, Muneta T, Hatsushika D, Horie M, Tsuji K, Kawarasaki T, Watanabe A, Hishikawa S, Fujimoto Y, Tanaka H, Kobayashi E: **Arthroscopic, histological and MRI analyses of cartilage repair after a minimally invasive method of transplantation of allogeneic synovial mesenchymal stromal cells into cartilage defects in pigs.** *Cytotherapy* 2012, **14**:327–338.
17. Adachi N, Sato K, Usas A, Fu FH, Ochi M, Han CW, Niyibizi C, Huard J: **Muscle derived, cell based ex vivo gene therapy for treatment of full thickness articular cartilage defects.** *J Rheumatol* 2002, **29**:1920–1930.
18. Benya P: **Dedifferentiated chondrocytes reexpress the differentiated collagen phenotype when cultured in agarose gels.** *Cell* 1982, **30**:215–224.

19. Takazawa K, Adachi N, Deie M, Kamei G, Uchio Y, Iwasa J, Kumahashi N, Tadenuma T, Kuwata S, Yasuda K, Tohyama H, Minami A, Muneta T, Takahashi S, Ochi M: **Evaluation of magnetic resonance imaging and clinical outcome after tissue-engineered cartilage implantation: prospective 6-year follow-up study.** *J Orthop Sci* 2012, **17**:413–424.
20. Adachi N, Ochi M, Deie M, Nakamae A, Kamei G, Uchio Y, Iwasa J: **Implantation of tissue-engineered cartilage-like tissue for the treatment for full-thickness cartilage defects of the knee.** *Knee Surg Sports Traumatol Arthrosc* 2014, **22**:1241–1248.
21. Nejadnik H, Hui JH, Feng Choong EP, Tai B-C, Lee EH: **Autologous bone marrow-derived mesenchymal stem cells versus autologous chondrocyte implantation: an observational cohort study.** *Am J Sports Med* 2010, **38**:1110–1116.
22. Peterson L, Minas T, Brittberg M, Lindahl A: **Treatment of osteochondritis dissecans of the knee with autologous chondrocyte transplantation: results at two to ten years.** *J Bone Joint Surg Am* 2003, **85-A**(Suppl 2):17–24.
23. Martin JA, Klingelhutz AJ, Moussavi-Harami F, Buckwalter JA: **Effects of oxidative damage and telomerase activity on human articular cartilage chondrocyte senescence.** *J Gerontol A Biol Sci Med Sci* 2004, **59**:324–337.
24. Rouwkema J, Koopman B, Blitterswijk C, Dhert W, Malda J: **Supply of nutrients to cells in engineered tissues.** *Biotechnol Genet Eng Rev* 2010, **26**:163–178.
25. Vasara AI, Hyttinen MM, Lammi MJ, Lammi PE, Långsjö TK, Lindahl A, Peterson L, Kellomäki M, Konttinen YT, Helminen HJ, Kiviranta I: **Subchondral bone reaction associated with chondral defect and attempted cartilage repair in goats.** *Calcif Tissue Int* 2004, **74**:107–114.

doi:10.1186/s13018-014-0098-z
Cite this article as: Ishihara *et al.*: Simultaneous regeneration of full-thickness cartilage and subchondral bone defects *in vivo* using a three-dimensional scaffold-free autologous construct derived from high-density bone marrow-derived mesenchymal stem cells. *Journal of Orthopaedic Surgery and Research* 2014 9:98.

The Veterinary Journal 202 (2014) 53–61

Contents lists available at ScienceDirect

The Veterinary Journal

journal homepage: www.elsevier.com/locate/tvjl

Multipotency of equine mesenchymal stem cells derived from synovial fluid

D. Murata [a], D. Miyakoshi [b], T. Hatazoe [c], N. Miura [a], S. Tokunaga [a], M. Fujiki [a], K. Nakayama [d], K. Misumi [a,*]

[a] Faculty of Veterinary Medicine, Kagoshima University, 21–24 Korimoto 1-chome, Kagoshima 890-0065, Japan
[b] Hidaka Horse Breeders Association, 175-2 Shizunai-Shinmori, Shinhidaka-cyo, Hidaka-gun, Hokkaido 056-0002, Japan
[c] Kyushu Stallion Station, The Japan Bloodhorse Bleeders' Association, 3995 Nagata, Osaki-cho, Soo-gun, Kagoshima 899-8313, Japan
[d] Graduate School of Science and Engineering, Saga University, 1 Honjyo-cho, Saga 840-8502, Japan

ARTICLE INFO

Article history:
Accepted 31 July 2014

Keywords:
Equine
Synovial fluid
Mesenchymal stem cells
Differentiation

ABSTRACT

Cartilage regeneration with cell therapy following arthroscopic surgery could be used in racehorses with intra-articular fractures (IAF) and osteochondritis dissecans (OCD). The aims of this study were to investigate the origin and multipotency of stromal cells in the synovial fluid (SF) of horses with intra-articular injury and synovitis, and to provide a new strategy for regeneration of lost articular cartilage. Mesenchymal stromal cells were isolated from SF of horses with IAF and OCD. Multipotency was analysed by RT-PCR for specific mRNAs and staining for production of specific extracellular matrices after induction of differentiation. The total number of SF-derived mesenchymal stromal cells reached $>1 \times 10^7$ by the fourth passage. SF-derived cells were strongly positive (>90% cells positive) for CD44, CD90 and major histocompatibility complex (MHC) class I, and moderately positive (60–80% cells positive) for CD11a/CD18, CD105 and MHC class II by flow cytometry. SF-derived cells were negative for CD34 and CD45. Under specific nutrient conditions, SF-derived cells differentiated into osteogenic, chondrogenic, adipogenic and tenogenic lineages, as indicated by the expression of specific marker genes and by the production of specific extracellular matrices. Chondrogenic induction in culture resulted in a change in cell shape to a 'stone-wall' appearance and formation of a gelatinous sheet that was intensely stained with Alcian blue. SF may be a novel source of multipotent mesenchymal stem cells with the ability to regenerate chondrocytes.

Introduction

Arthroscopic surgery to remove osteochondral fragments and to curette the surrounding degenerative cartilage has been accepted worldwide in Thoroughbred horses with intra-articular fractures (IAFs) and osteochondritis dissecans (OCD). To repair defects with hyaline cartilage, cartilage regeneration using mesenchymal stem cells (MSCs) derived from bone marrow (BM) (Arnhold et al., 2007) or adipose tissue (AT) (Braun et al., 2010) has been investigated.

The advantage of AT-MSCs is the abundance of MSCs per unit weight of tissue (Burk et al., 2013). However, we believe that a therapeutic strategy using AT-MSCs may be unacceptable in racehorse practice, because of the lower somatic fat quantities in Thoroughbred horses compared to Standardbred horses (Kearns et al., 2001). Paracentesis to aspirate BM is invasive and must be done with care to avoid contamination (Vidal et al., 2007).

Stem cells are increased in the synovial fluid (SF) of human beings with joint disease and injury (Jones et al., 2004; Morito et al., 2008). Improved clinical outcomes have been reported following treatment of cartilage deficits in human beings using MSCs derived from the synovium and SF (Nimura et al., 2008; Lee et al., 2011; Sekiya et al., 2012; Suzuki et al., 2012). If MSCs can be isolated from SF and expanded over a short time period after a racehorse is injured, they may be useful as a new strategy for cartilage regeneration. The aims of this study were to investigate the proliferative capacity, phenotypic characteristics and multipotency of cells in the SF associated with intra-articular injury and synovitis, and to provide a new strategy for regenerating lost or damaged cartilage with SF-MSCs.

Materials and methods

Samples

SF (3–4 mL per joint) was collected aseptically from the carpal, fetlock or tarsal joints of 11 Thoroughbred horses with IAF or OCD at the time of arthroscopic surgery (Table 1). SF samples were also obtained from nine diseased and nine normal Thoroughbred horse joints to compare the number of MSCs in the SF (Table 2). AT and BM were collected from two other horses (a male aged 10 years and a female aged

* Corresponding author. Tel.: +81 99 2858731.
E-mail address: kaz_msm@vet.kagoshima-u.ac.jp (K. Misumi).

http://dx.doi.org/10.1016/j.tvjl.2014.07.029
1090-0233/

Table 1
Profiles of synovial fluid (SF) samples obtained from the joints of horses with intra-articular fractures (IAFs) or osteochondritis dissecans (OCD).

Sample number	Age (years)	Sex	Disease	Diseased site (limb/joint)	Period of clinical onset (weeks)
1	3	F	IAF	RF/Carpus	2
2	2	F	IAF	RF/Fetlock	4
3	2	F	IAF	LF/Fetlock	4
4	1	F	IAF	LH/Tarsus	3
5	1	F	OCD	LH/Tarsus	3
6	3	M	IAF	RF/Carpus	2
7	3	F	IAF	RF/Carpus	2
8	3	M	IAF	RF/Carpus	2
9	3	M	IAF	RF/Carpus	2
10	6	M	IAF	RH/Tarsus	2
11	1	F	OCD	LH/Tarsus	No signs

SF samples were aseptically obtained from carpal, fetlock or tarsal joints of 11 Thoroughbred horses with IAF or OCD. M, male; F, female; RF, right forelimb; LF, left forelimb; RH, right hind limb; LH, left hind limb.

3 years) that were free of any joint diseases. All procedures were approved by the Animal Care and Use Committee of Kagoshima University (approval number A11037; date of approval 26 March 2012).

Isolation and expansion of stromal cells from synovial fluid

SF was diluted with five volumes of phosphate buffered saline (PBS), filtered through a 70 μm nylon filter (Cell Strainer, BD Falcon) to remove debris and centrifuged at 160 *g* for 5 min at room temperature. After decanting the supernatant, the pellet was resuspended and plated in a 25 cm^2 culture flask in complete culture medium (CCM) consisting of Dulbecco's Modified Eagle's Medium (DMEM, Life Technologies), 10% fetal bovine serum (FBS, Thermo Scientific) and 1% antibiotic-antifungal preparation (100 U/mL Penicillin G, 100 μg/mL streptomycin, 0.25 μg/mL amphotericin B; Antibiotic-Antimycotic, Life Technologies). After incubation at 37 °C in 5% CO_2 for 9 days, cells adhering to the bottom of the flask were washed with PBS and harvested as described below. The medium was changed on days 4 and 7 (D7; Passage 0, P0). The number of colonies was counted at P0 in the 18 SF samples from the nine diseased and nine normal horse joints (Table 2).

Cultured cells were harvested with 0.05% trypsin and 0.2 mM ethylene diamine tetraacetic acid (Trypsin-EDTA, Life Technologies), and centrifuged. After decanting the supernatant, the pellet was rinsed with CCM and the cells were replated at 1×10^6 cells in 150 cm^2 dishes and cultured for 9 days. The medium was changed every 3 days for 9 days (P1). This serial process of passaging was repeated to obtain $>1 \times 10^7$ cells for reverse transcription (RT)-PCR and flow cytometry. The total number of cells was determined with a cell counter at every passage from P1 to determine proliferation rates, which were calculated as the cell doubling number, cell doubling time and daily duplication rate using the following formulas:

$$\text{Cell doubling number} = \ln(\text{final number of cells}/\text{initial number of cells})/\ln(2)$$

$$\text{Cell doubling time} = \text{Cell culture time}/\text{cell doubling number}$$

$$\text{Daily duplication rate} = \text{Cell doubling number}/\text{cell culture time} = 1/\text{cell doubling time}$$

Surface markers and multipotency of the cells were analysed at the fifth passage (P5). Normal SF-MSCs were analysed at P6, when sufficient numbers of cells were obtained.

Isolation and expansion of stromal cells from adipose tissue and bone marrow

Horses were sedated by IV injection with 4 μg/kg medetomidine HCl (Domitor, Zenoaq) and 10 μg/kg butorphanol tartrate (Vetorphale, Meiji Seika), and 25–30 g AT were obtained from the gluteal subcutis using liposuction. Liposuction solution (100–200 mL) consisting of physiological saline (Normal Saline, Otsuka) containing 400 μg/mL lignocaine HCl and 0.4 μg/mL adrenaline (Xylocaine injection 1% with Epinephrine, AstraZeneca) was injected SC through a 10 mm skin incision and AT was aspirated with a probe (Collection Cannula, 14 G, length 30 cm; Cytori) connected to a 50 mL syringe. This procedure was repeated 10 times. The aspirated AT was digested with a 2× volume of PBS containing 0.1% collagenase (Life Technologies) at 37 °C for 90 min, filtered through a 70 μm nylon filter (Cell Strainer, BD Falcon) and centrifuged at 160 *g* for 5 min at room temperature. The cell pellet was re-suspended in CCM and incubated at 37 °C in 5% CO_2 for 9 days, then cells adhering to the bottom of the flask were washed with PBS and harvested. The medium was changed on the day 6 (D6; P0).

BM (30–35 mL) was collected from the fifth segment of the sternum by needle core biopsy under local anaesthesia with 20 mg/mL lignocaine HCl (Xylocaine Injection 2%, AstraZeneca) and the same sedatives and analgesics as used for AT collection. A bone marrow biopsy needle (11 G, length 10.2 cm; Angiotech) was inserted through a 10 mm skin incision. BM was aspirated with a 20 mL syringe containing 5000 IU heparin, then re-suspended in CCM. After incubation at 37 °C in 5% CO_2 for 9 days, the cells adhering to the bottom of the flask were washed with

Table 2
Colonies of normal and diseased equine synovial fluid (SF)-derived mesenchymal stem cells at passage 0.

Source of stem cells	Sample number	Disease	Limb/Joint	Colonies at passage 0	Mean ± standard deviation	*P* value
SF from diseased joints	D1	IAF	RF/Carpus	73	166.9 ± 100.9	0.001
	D2	IAF	RF/Carpus	62		
	D3	IAF	LF/Carpus	94		
	D4	IAF	RF/Carpus	121		
	D5	IAF	LF/Carpus	364		
	D6	IAF	RF/Carpus	271		
	D7	OCD	RH/Tarsus	161		
	D8	IAF	RF/Carpus	136		
	D9	IAF	RF/Carpus	220		
SF from normal joints	N1	ND	LF/Carpus	10	8.3 ± 6.5	
	N2	ND	LF/Carpus	21		
	N3	ND	LF/Carpus	10		
	N4	ND	RF/Carpus	5		
	N5	ND	LF/Carpus	6		
	N6	ND	LH/Tarsus	3		
	N7	ND	RF/Carpus	5		
	N8	ND	RH/Tarsus	0		
	N9	ND	LF/Carpus	13		

SD, standard deviation; IAF, intra-articular fractures; OCD, osteochondritis dissecans; ND, no data; RF, right forelimb; LF, left forelimb; RH, right hind limb; LH, left hind limb.

Table 3
Reverse transcriptase PCR primer sequences, annealing temperatures and amplification product sizes for multipotent, osteogenic, chondrogenic, adipogenic and tenogenic genes.

Marker	Gene	Sequence (Forward/Reverse)	Annealing temperature (°C)	Fragment (base pairs)
Multipotency	Nanog	5′-TACCTCAGCCTCCAGCAGAT-3′ 5′-CATTGGTTTTTCTGCCACCT-3′	58.0	190
	Sox2	5′-TGGTTACCTCTTCCTCCCACT-3′ 5′-GGGCAGTGTGCCGTTAAT-3′	58.0	179
Osteogenesis	Runx2	5′-TGTCATGGCGGGTAACGAT-3′ 5′-TCCGGCCCACAAATCTCA-3′	61.3	107
	ALP	5′-GCTGGGAAATCCGTGGGCATTGTG-3′ 5′-CGGCAGAGTGGGCGTAGG-3′	64.3	81
	OC	5′-GAGGGCAGTGAGGTGGTGAAG-3′ 5′-CTCCTGGAAGCCGATGTGGTC-3′	63.3	152
Chondrogenesis	Sox9	5′-AGTACCCGCACCTGCACAAC-3′ 5′-CGCTTCTCGCTCTCGTTCAG-3′	50.0	79
	Col-2	5′-GCTTCCACTTCAGCTATGGA-3′ 5′-TGTTTCGTGCAGCCATCCTT-3′	56.9	256
	AGG	5′-TGCACAGACCCCGCCAGCTA-3′ 5′-GTCTCTAAACTCAGTCCACG-3′	51.4	339
Adipogenesis	PPARγ2	5′-GTCTCATAACGCCATCAGGTTTG-3′ 5′-GCCCTCGCCTTCGCTTTG-3′	50.0	180
Tenogenesis	Scx	5′-TCTGCCTCAGCAACCAGAGA-3′ 5′-TCCGAATCGCCGTCTTTC-3′	58.0	59
	TenC	5′-GATCTTCACTTCCCTACCAACG-3′ 5′-CTCATCCAGCATGGGGTC-3′	58.0	70
Housekeeping	GAPDH	5′-ACCACAGTCCATGCCATCAC-3′ 5′-TCCACCACCCTGTTGCTGTA-3′	60.0	450

Nanog, homeobox protein NANOG; Sox2, sex determining region Y-box 2; GAPDH, glyceraldehyde-3-phosphate dehydrogenase; ALP, alkaline phosphatase; OC, osteocalcin; Sox9, sex determining region Y-box 9; Col-II, type II collagen; AGG, aggrecan; PPARγ2, peroxisome proliferator activated receptor γ2; Scx, scleraxis; TenC, tenascin C.

PBS and harvested as described above. The medium was changed on the day 6 (D6; P0).

Expression of multipotency markers by stromal cells from synovial fluid

Total RNA from cultured cells was isolated using the mirVana miRNA Isolation Kit (Life Technologies) and converted to cDNA by RT using the TaKaRa RT-PCR system (PCR Thermal Cycler MP, TaKaRa) and RT-PCR kit (ReverTra Dash, Toyobo), with a 20 min incubation at 42 °C, followed by a 5 min incubation at 99 °C to inactivate the RT. PCR primers and expected sizes of products for homeobox protein Nanog and sex determining region Y-box 2 (Sox2) are summarised in Table 2. PCR conditions were 30 cycles of 98 °C for 10 s, individual annealing temperature for 2 s (Table 3) and 74 °C for 15 s. The reaction products were separated by electrophoresis on 1.5% agarose gels and the expression of multipotency markers was determined based on the expected size of the bands labelled with SYBR green.

Flow cytometry

Cells (1×10^4) were resuspended in 500 μL staining buffer (SB; PBS containing 1% FBS) and incubated for 30 min at 4 °C with 20 μg/mL antibodies that recognise CD11a/CD18, CD34, CD44, CD45, CD90, CD105 and major histocompatibility complex (MHC) classes I and II (Table 4). Prior to incubation with cells, antibodies against CD11a/CD18, CD44 and MHC classes I and II were coupled with secondary antibodies conjugated to fluorescein isothiocyanate (FITC). Non-specific FITC mouse immunoglobulin G1κ was used as a negative control. FITC-labelled cells were washed with SB and resuspended in 500 μL SB for fluorescence-activated cell sorting (FACS). Cell fluorescence was evaluated as a strong shift in the mean fluorescence intensity (MFI) by flow cytometry using a FACS Aria II instrument. The data were analysed using FACS Diva software.

Induction and evaluation of differentiation

To investigate osteogenic differentiation, cells were plated in 6-well plates (6 Well Plate-N, Nest Biotech) in CCM at an initial density of 2.5×10^3 cells/cm^2. After 24 h incubation, CCM was replaced with osteogenic induction medium (Differentiation Basal Medium-Osteogenic, Lonza) supplemented with 100 μM ascorbic acid, 10 mM β-glycerophosphate and 1 μM dexamethasone. After 2 weeks in induction medium, total RNA from the plate-cultured cells was prepared as described above and expression of the osteoblast-specific genes runt-related transcription factor 2 (Runx2), alkaline phosphatase (ALP) and osteocalcin (OC) were analysed. PCR primers, amplification conditions and the expected sizes of the products are summarised in Table 3. Negative controls for RT-PCR products were obtained from SF-derived stromal cells that were not placed in induction medium (data not shown).

Chondrogenic differentiation was induced in aggregate and plate cultures for 2 weeks. Cells (5×10^5) were resuspended in a 15 mL centrifuge culture tube (SuperClear Centrifuge Tubes, Labcon) in 500 μL chondrogenic induction medium (Differentiation Basal Medium-Chondrogenic, Lonza) supplemented with 4.5 g/L D-glucose, 350 μM L-proline, 100 nM dexamethasone and 0.02 g/L transforming growth factor (TGF)-β3. Another aliquot of 5×10^4 cells was resuspended in a 6-well plate in 2 mL induction medium, which was replaced three times per week, similar to osteogenic induction. Two weeks later, total RNA from the plate-cultured cells was prepared as described above and expression of chondrogenic marker genes, including sex determining region Y-box 9 (Sox9), type II collagen (Col-II) and aggrecan, was examined (Table 3). Production of mucopolysaccharide in the chondrogenic extracellular matrix

Table 4
Antibodies for analysing the specific molecular markers on the cell surface.

Antibody	Company	Clone	Epitope	Dilution
CD11a/CD18	Gift[a]	CZ3.2, 117, 2E11, B10	Not confirmed	1:10
CD34	BD Bioscience	581/CD34	O-glycosylated transmembrane glycoprotein	1:5
CD44	AbD Serotec	CVS18	Not confirmed	1:10
CD45	BD Bioscience	2D1	T200 family	1:2.5
CD90	BD Bioscience	5E10	Not confirmed	1:10
CD105	AbD Serotec	SN6	Glycoprotein homodimer	1:10
MHC class I	Gift[a]	CZ3, 117, 1B12, C11	Not confirmed	1:10
MHC class II	Gift[a]	CZ11, 130, 8E8, D9	Not confirmed	1:10
Secondary (FITC)	Rockland	–	Mouse IgG (H and L)	1:500
Isotype control	BD Bioscience	MOPC-21	Not confirmed	1:10

[a] The antibodies against CD11a/18 and MHC classes I and II were gifts from Dr Douglas Antczak, Cornell University, Ithaca, New York, USA. MHC, major histocompatibility complex; FITC, fluorescein isothiocyanate.

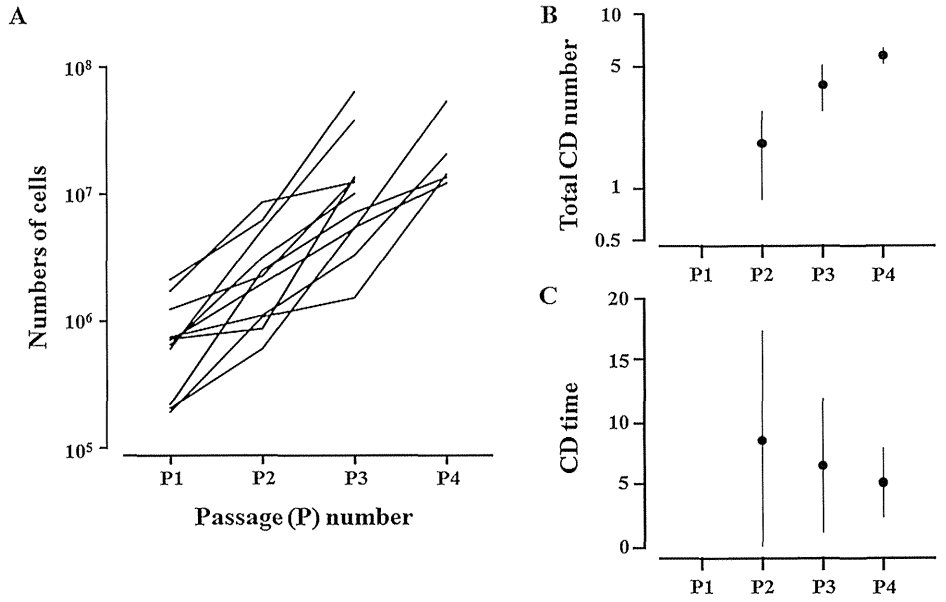

Fig. 1. Growth curves (a), total cell doubling numbers (b) and cell doubling (CD) times (c) from passages 0 to 4 (P0–P4) of synovial fluid (SF)-derived mesenchymal stem cells (MSCs) collected from 11 horses. Six samples produced >1 × 10^7 cells at P3 and five samples required ~6 weeks to reach >1 × 10^7 cells (at P4). CD number = ln(Nf / Ni) / ln(2). *CD time = cell culture time / CD number. Nf, final number of cells; Ni, initial number of cells.*

was determined by staining with Alcian blue in 6-well plates. The differentiated cells were fixed onto the culture plate by methanol, then treated with 3% acetic acid. The plates onto which the cells adhered were stained with Alcian blue (pH 2.5) for 90 min.

Cell aggregates were fixed with 10% neutral buffered formalin, dehydrated in graded series of ethanol, embedded in paraffin, sectioned at 5 μm thickness and mounted on glass slides. After dehydration with methanol and treatment with 3% acetic acid, cell aggregates were stained with Alcian blue (pH 2.5) for 90 min to detect cartilage-specific proteoglycans, then counterstained with Mayer's haematoxylin. The sections were also analysed immunohistochemically with an antibody against cartilage oligomeric matrix protein (COMP; catalogue number ab91354, Abcam). Following deparaffinisation and rehydration, the sections were treated with blocking buffer (0.01 M PBS containing 0.25% casein), then incubated with primary antibody (diluted 1:100 in blocking buffer) overnight. The slides were incubated with secondary biotinylated goat anti-rabbit IgG (Polyclonal Goat Anti-Rabbit Immunoglobulins/Biotinylated; catalogue number E0432, DakoCytomation; diluted 1:300), for 30 min. Secondary antibodies were labelled with avidin-biotin-horseradish peroxidase complex (ABC standard kit, VectaStain) and visualised after treatment with 3, 3′-diaminobenzine.

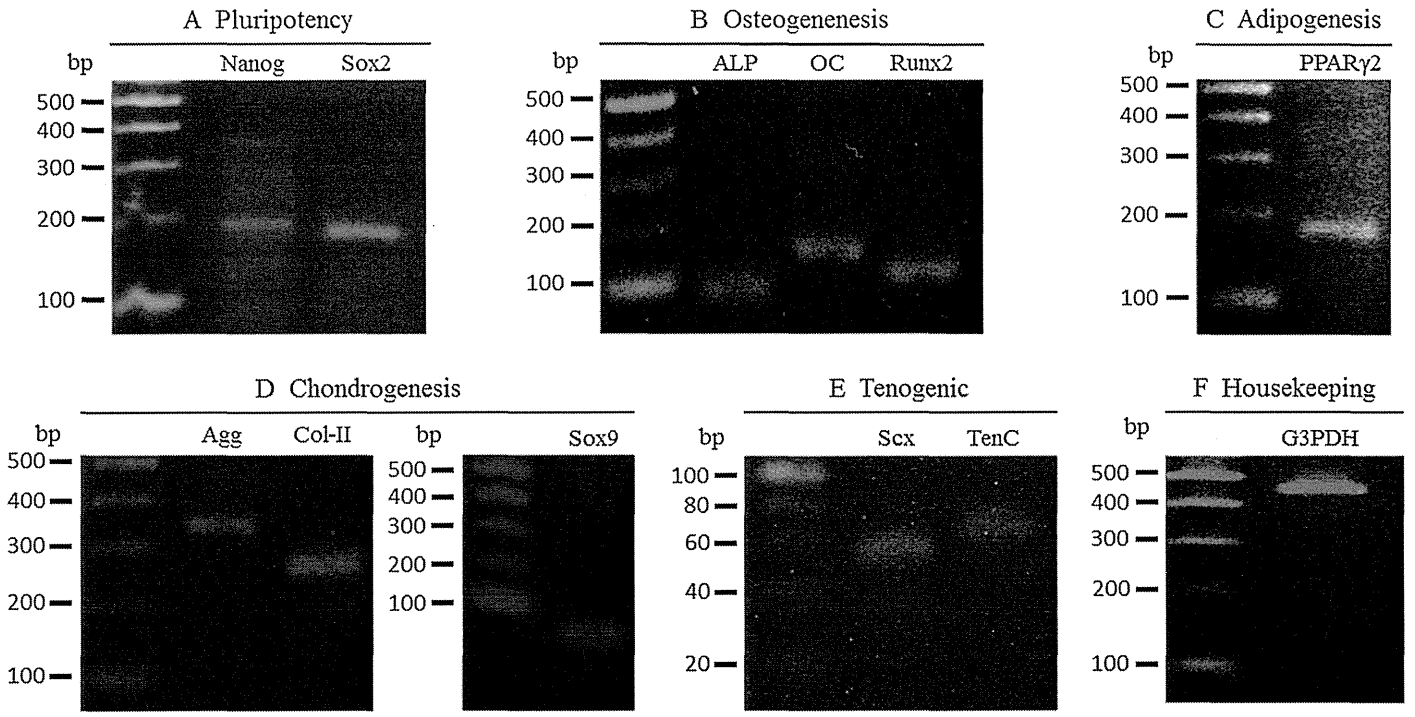

Fig. 2. Results of reverse transcriptase-PCR using specific marker genes of multipotency, and osteogenic, chondrogenic, adipogenic and tenogenic differentiation. Nanog, homeobox protein NANOG; Sox2, sex determining region Y-box 2; Runx2, runt-related transcription factor 2; ALP, alkaline phosphatase; OC, osteocalcin; Sox9, sex determining region Y-box 9; Col2, type II collagen; Agg, aggrecan; PPARγ2, peroxisome proliferator activated receptor γ2; Scx, scleraxis; TenC, tenascin C; G3PDH, glyceraldehyde-3-phosphate dehydrogenase.

Table 5
Percentages (%) of positive cells to specific molecular markers by flow cytometry.

	Diseased SF-MSCs	Normal SF-MSCs	BM-MSCs	AT-MSCs
CD11a/CD18	73.7 ± 2.3	61.6 ± 3.2	80.1 ± 1.1	79.6 ± 5.5
CD34	0.3 ± 0.2	0.3 ± 0.2	0.4 ± 0.1	1.0 ± 0.2
CD44	98.1 ± 0.6	97.9 ± 0.5	96.8 ± 0.0	95.6 ± 2.4
CD45	0.2 ± 0.1	0.2 ± 0.1	0.4 ± 0.1	1.0 ± 0.8
CD90	99.0 ± 0.4	96.0 ± 3.7	98.5 ± 0.7	98.7 ± 0.8
CD105	73.5 ± 6.0	77.9 ± 1.6	50.2 ± 27.2	77.1 ± 14.5
MHC-1	94.6 ± 3.3	95.9 ± 1.6	90.8 ± 6.5	94.5 ± 2.6
MHC-II	71.9 ± 4.1	74.9 ± 3.0	78.1 ± 3.9	79.3 ± 7.7

SF, synovial fluid; BM, Bone marrow; AT, adipose tissue; MSCs, mesenchymal stem cells; MHC, major histocompatibility complex.

Adipogenic differentiation was induced when cells reached a density of 15,000 cells/cm^2 on 6-well plates in basal medium. After pre-incubation for 24 h, CCM was replaced with adipogenic induction medium, composed of DMEM supplemented with 4.5 g/L D-glucose, 100 μM indomethacin, 10 μg/mL insulin, 0.5 mM 3-isobutyl-1-methylxanthine, 1 μM dexamethasone and 5% rabbit serum. Seven days later, total RNA from the cells was isolated as described above and evaluated for expression of the adipogenic marker gene peroxisome proliferator activated receptor γ2 (PPARγ2) (Table 3). Adipocyte-specific intracellular lipids were stained with oil red O.

Tenogenic differentiation was induced when cells reached a density of 15,000 cells/cm^2 on 6-well plates in CCM. After incubation for 24 h, 50 ng/mL bone morphogenetic protein (BMP) 12 (Recombinant Human BMP-12/GDF-7, BioVision) was added to CCM for tenogenic induction. Following 2 weeks in induction medium, total RNA from the plate-cultured cells was prepared as described above, and expression of scleraxis (Scx) and tenascin C (TenC) as tenocyte- and tenogenesis-specific genes were analysed (Table 3).

Statistical analysis

All quantitative group data are shown as the mean ± standard deviation (SD). Data were analysed using Student's *t* test (Excel, Microsoft). Differences of $P < 0.01$ were considered to be statistically significant.

Results

Isolation and expansion of stromal cells

SF-derived MSCs adhering to the bottom of the culture flask were spindle-shaped and present as a minority of the cell components. At P0, the total number of colonies of SF-MSCs from diseased joints

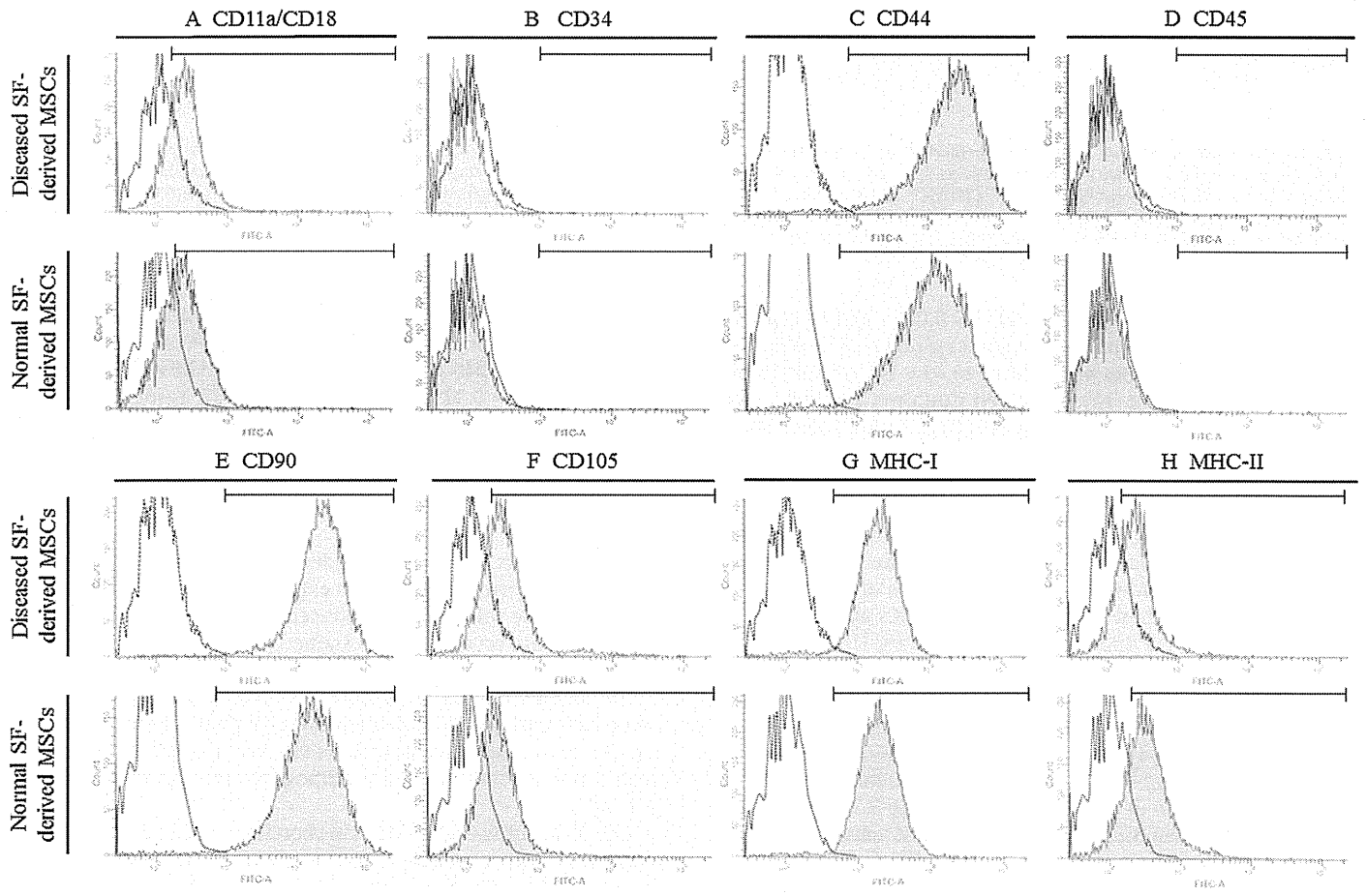

Fig. 3. Results of flow cytometry using immunological markers on synovial fluid (SF)-derived mesenchymal stem cells (MSCs) from normal and diseased joints. A strong shift in mean fluorescence intensity (MFI) was detected with antibodies against CD44 (C), CD90 (E) and major histocompatibility complex (MHC) class I (G); a positive signal with antibodies against CD11a/18 (A), CD105 (F) and MHC class II (H) partially overlapped with the negative control; no positive signal was detected with antibodies against CD34 (B) and CD45 (D). The dotted line represents the negative control. The horizontal line in individual histograms indicates the population of the positive cells.

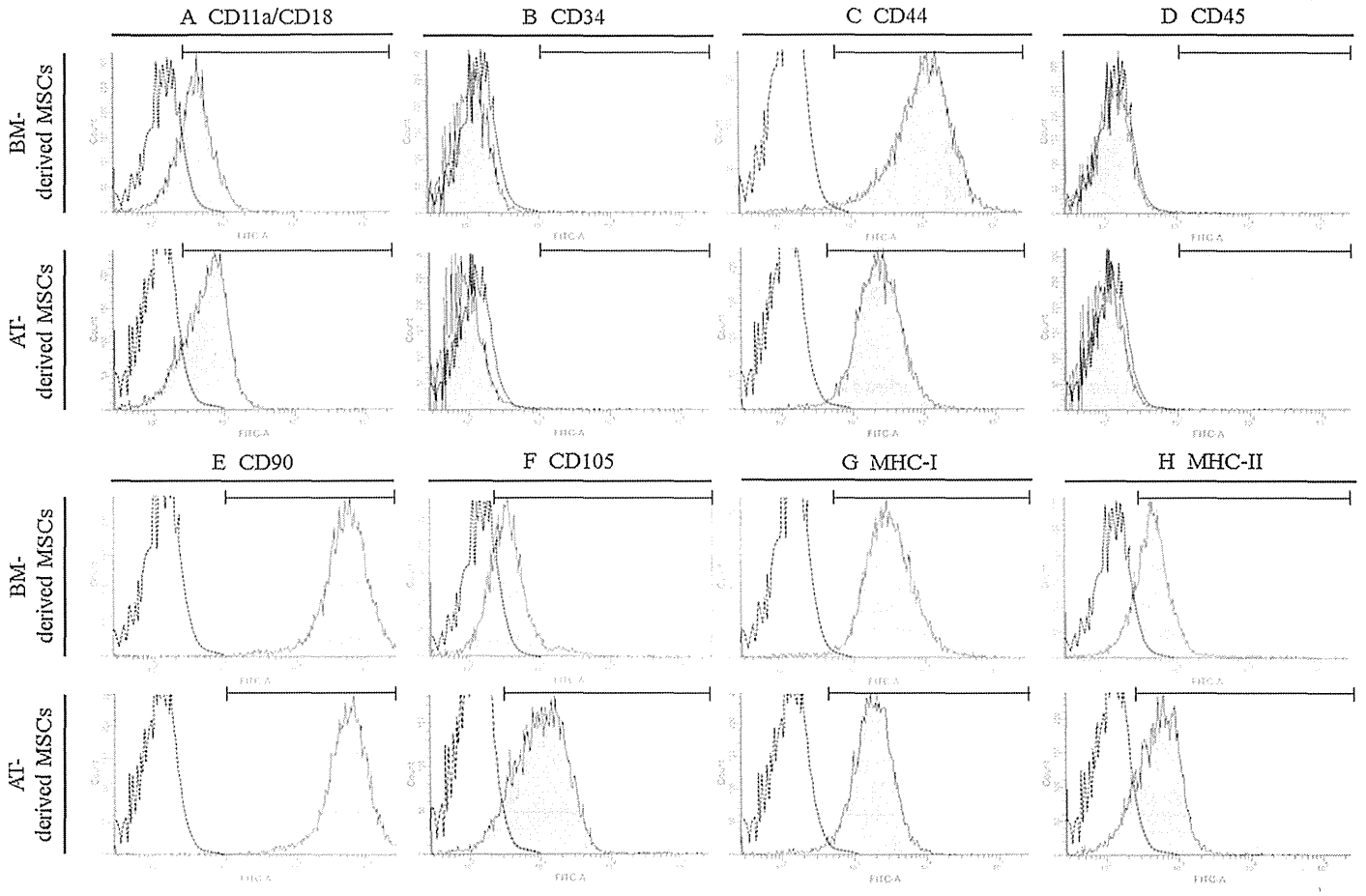

Fig. 4. Results of flow cytometry using the same markers as in Fig. 3 on adipose tissue (AT)-derived and bone marrow (BM)-derived mesenchymal stem cells (MSCs). A strong shift in mean fluorescence intensity (MFI) was detected with antibodies against CD44 (C), CD90 (E) and major histocompatibility complex (MHC) class I (G); a positive signal with antibodies against CD11a/18 (A), CD105 (F) and MHC class II (H) partially overlapped with the negative control; no positive signal was detected with antibodies against CD34 (B) or CD45 (D). The dotted line represents the negative control. The horizontal line in individual histograms indicates the population of the positive cells. The signal patterns were similar to those in synovial fluid (SF)-derived MSCs.

(62–364 colonies) was significantly ($P = 0.001$) higher than the number from normal joints (0–21 colonies) (Table 2). SF-MSCs isolated from diseased joints proliferated to $>1 \times 10^6$ cells at P3 and 1×10^7 cells at P4 (Fig. 1a). Total cell doubling numbers were 1.81 ± 0.94, 3.93 ± 1.11 and 5.83 ± 0.54 at P2, P3 and P4, respectively (Fig. 1b). Daily duplication rates were 0.20 ± 0.11, 0.23 ± 0.12 and 0.25 ± 0.11 at P2, P3 and P4, respectively (see Appendix: Supplementary Fig. S1).

AT-MSCs and BM-MSCs could be transferred repeatedly to the next passage at intervals of 6 days, whereas the interval for SF-MSCs was 9 days. However, the doubling times of SF-MSCs were not significantly different from those of AT-MSCs and BM-derived MSCs (BM-MSCs) (see Appendix: Supplementary Fig. S2).

Reverse transcription-PCR and flow cytometry of stromal cells

Positive expression of Nanog and Sox2 in SF-MSCs was confirmed by RT-PCR (Fig. 2a). Expression of immunological markers on SF-MSCs is shown in Figs. 3 and 4, and Table 5. More than 90% of cells were positive for CD44, CD90 and MHC class I (Figs. 3c, e and g) and 60–80% of cells were positive for CD11a/18, CD105 and MHC class II, overlapping with the negative control (Figs. 3a, f and h), whereas no signal was detected with antibodies against CD34 and CD45 (Figs. 3b and d). Equine mononuclear blood cells were positive for CD34 and CD45 (see Appendix: Supplementary Fig. S3), as previously reported (Barberini et al., 2014; Mohanty et al., 2014).

No statistical difference in flow cytometry was observed between the SFs from the normal and diseased joints (P values for CD11a/18, CD34, CD44, CD45, CD90, CD105, MHC-I and MHC-II were 0.013, 0.714, 0.7, 0.768, 0.317, 0.372, 0.639 and 0.45, respectively). The results of SF-MSCs corresponded to those of AT-MSCs and BM-MSCs (Fig. 4).

Differentiation

After 2 weeks of osteogenic induction, SF-MSCs aggregated and contracted to form colonies, with expression of Runx2, ALP and OC (Fig. 2b). These cell clusters produced a specific matrix, including calcium apatite crystals, which stained positively with alizarin red (Fig. 5a, negative control is shown in Fig. 6a).

Adipogenic induction of MSCs resulted in adipocyte-like flattened cells with small lipid vesicles that stained positively with oil red O (Fig. 5b, negative control is shown in Fig. 6b). RT-PCR revealed the expression of the adipogenic marker gene PPAR-γ2 (Fig. 2c).

The plate culture of SF-MSCs in chondrogenic induction medium induced a change in cell shape to a 'stone-wall' structure, followed by formation of a gelatinous monolayer that stained intensely with Alcian blue (Fig. 5c, negative control is shown in Fig. 6c). Blue sheets were also formed by chondrogenic induction of SF-MSCs at P10 (Fig. 7a) and SF-MSCs from normal joints (Fig. 7b). However, AT-MSCs and BM-MSCs formed no blue gelatinous sheets

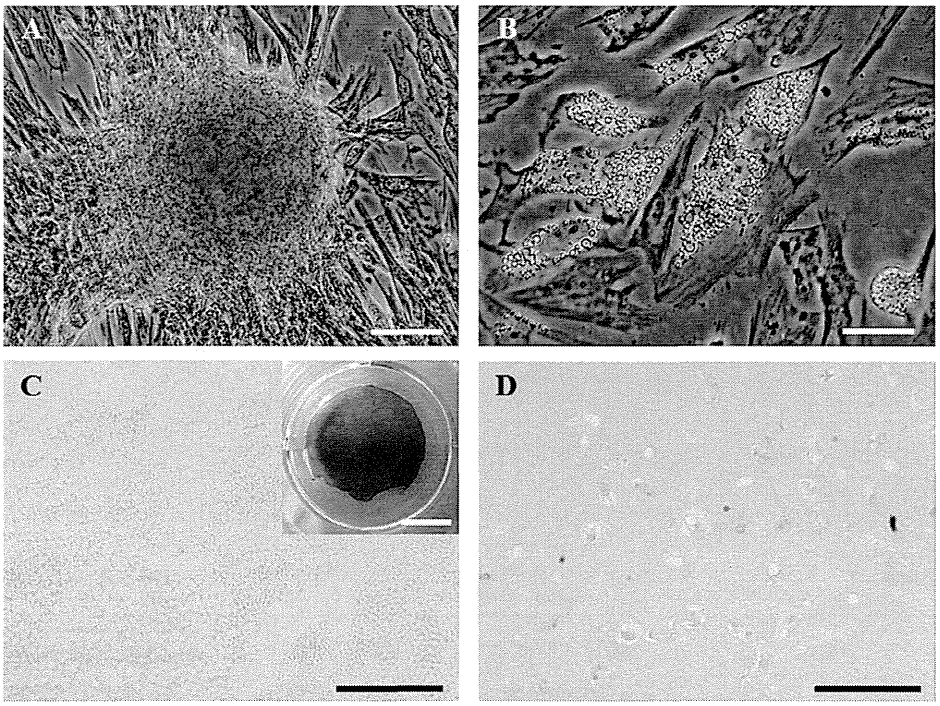

Fig. 5. Representative images showing staining with alizarin red for osteogenic differentiation (A), oil red O for adipogenic differentiation (B) and Alcian blue for chondrogenic differentiation (C and D) of synovial fluid (SF)-derived mesenchymal stem cells (MSCs). Following 2 weeks of osteogenic induction, the SF-MSCs aggregated and contracted to form colonies, and produced a specific matrix including calcium apatite crystals, which were positively stained with alizarin red. Scale bar = 100 μm (A). Adipogenic induction of SF-MSCs resulted in adipocyte-like flattened cells with small lipid vesicles that stained red with oil red O. Scale bar = 50 μm (A). Plate culture of SF-MSCs in chondrogenic induction medium induced a change in cell shape into a 'stone-wall' structure. Scale bar = 500 μm. A gelatinous monolayer sheet was present that intensely stained with Alcian blue. Scale bar = 1 cm in the inset picture (C). Histological preparation of cell pellets showing a hyaline cartilage-like structure that was positively stained with Alcian blue. Scale bar = 100 μm (D).

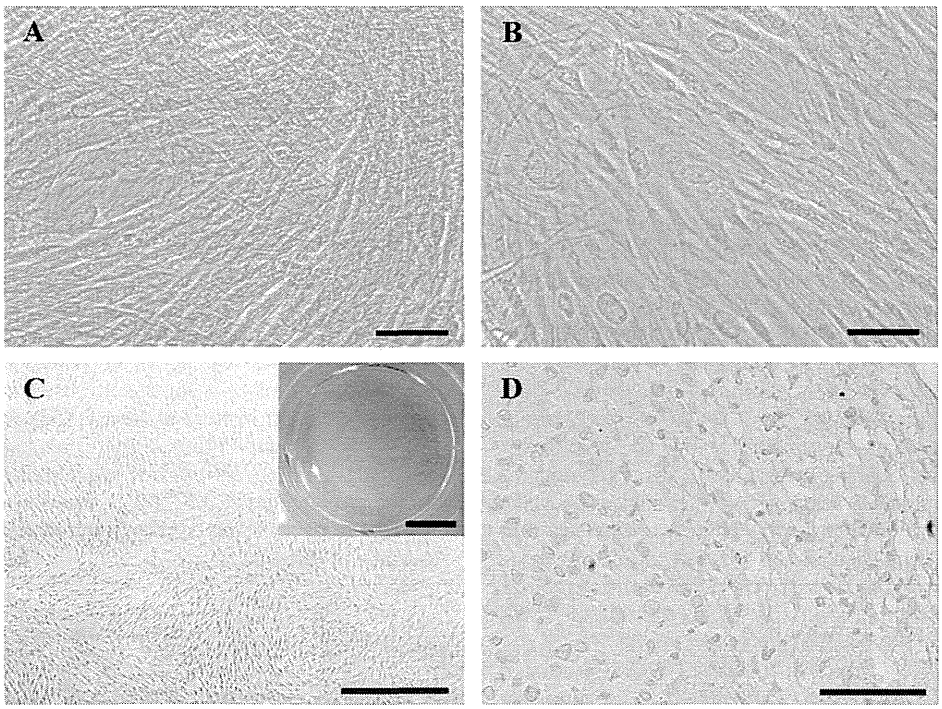

Fig. 6. Representative images showing synovial fluid (SF)-derived mesenchymal stem cells (MSCs) stained with alizarin red (A), oil red O (B) and Alcian blue (C and D). The negative controls were cultured with complete culture medium (CCM) during the corresponding periods of time taken to induce osteogenic, adipogenic and chondrogenic differentiation (A–C). The negative control for the cell pellet (D) was cultured in chondrogenic induction medium without transforming growth factor (TGF)-β3. Positive staining was not seen in (A) or (B) and no gelatinous monolayer sheet was formed (D). Chondrocyte and hyaline matrices were not seen in the pellet (D).

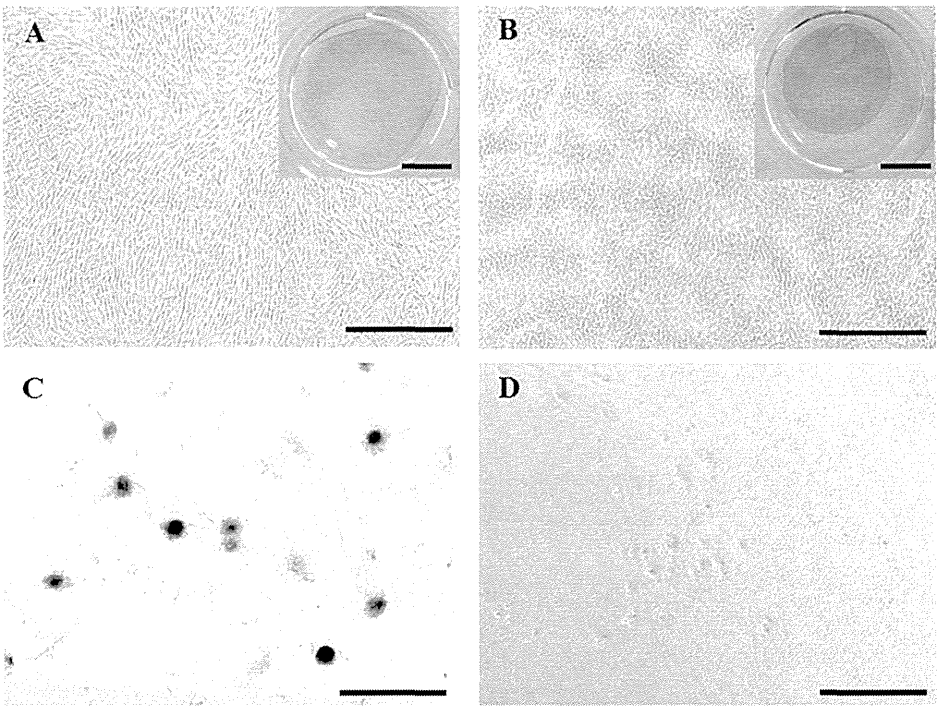

Fig. 7. Representative images showing Alcian blue staining of plate cultures of synovial fluid (SF)-derived mesenchymal stem cells (MSCs), adipose tissue (AT)-derived MSCs and bone marrow (BM)-derived MSCs after chondrogenic induction. Staining of the gelatinous sheets in SF-MSCs was intensely blue at passage 10 (P10) from the diseased joints (A), as well as SF-MSCs from the normal joints (B). Blue sheets were not formed following chondrogenic induction of AT-MSCs and BM-MSCs (C and D). Scale bar = 500 μm.

following chondrogenic induction (Figs. 7c and d). RT-PCR revealed elevated expression of marker genes specific for chondrogenesis, including Sox-9, Col-II and aggrecan (Fig. 2d). Histological observation of the cell pellets showed a hyaline cartilage-like structure that was positively stained with Alcian blue (Fig. 5d, negative control is shown in Fig. 6d) and which abundantly expressed cartilage-specific molecules, such as COMP in the extracellular matrix (see Appendix: Supplementary Fig. S4). RT-PCR revealed the expression of tenogenic marker genes, such as Scx and TenC (Fig. 2e).

Discussion

In the present study, equine SF from joints with osteochondral fragments included spindle-shaped cells that adhered to culture dishes and proliferated to form colonies; these findings correspond to the distinctive features of human MSCs (Friedenstein, 1976). Previously defined markers for MSCs, in which CD44, CD90 and CD105, but not CD34 or CD45, are expressed (Morito et al., 2008; Sekiya et al., 2012), were identical in the cells derived from equine SF, as well as equine AT-MSCs and BM-MSCs, in the present study. In addition to these results, the ability of these cells to differentiate into osteoblasts, chondrocytes, adipocytes and tenocytes was also a feature of equine SF-MSCs, as well as equine AT-MSCs and BM-MSCs. If we can efficiently and effectively isolate and increase the number of cells, SF could be a useful source of equine MSCs for equine cartilage regeneration, since arthrocentesis to collect SF is less invasive and has a lower risk of contamination with infectious agents compared to collection of BM or AT.

In this study, we used SF from injured joints, which produced small numbers of colonies of MSCs at P0 and reached a total number of $>1 \times 10^5$ cells at P1. In a human study, MSCs were detected at very low densities in SF from normal volunteers, but increased with the grade of osteoarthritis (Sekiya et al., 2012). In the present study, we showed that the number of colonies of SF-MSCs at P0 was significantly increased in equine SF from diseased joints compared to normal joints. Since fewer MSCs are present in normal SF, the increased numbers of the cells in SF from diseased or injured joints suggest that SF-MSCs could play a role in the process of degradation, repair and regeneration of damaged cartilage. On the basis of morphology and gene profile, SF-MSCs were more similar to synovium-derived MSCs than to BM-MSCs (Sekiya et al., 2012). Another study suggested that human SF-MSCs are released from the synovium in association with joint insults (Nimura et al., 2008); we speculate that equine SF-MSCs may be released from the synovium, especially in cases of OCD.

In our study, plate culture of SF-MSCs from normal or diseased joints in chondrogenic induction medium induced a change in the cell shape to a 'stone-wall' structure typical of chondrogenic differentiation, followed by formation of a gelatinous monolayer that was intensely stained with Alcian blue. However, chondrogenic induction of AT-MSCs and BM-MSCs resulted in no blue gelatinous sheet. A previous report suggested that SF-MSCs may be a superior source of cells for autologous transplantation for cartilage regeneration in human beings (Sakaguchi et al., 2005). Our results suggest that equine SF might be a superior source of MSCs for cartilage regeneration, but more definitive results would be needed to conclude that SF-MSCs could be suitable for generating cartilage matrix during chondrogenic differentiation compared to AT-MSCs or BM-MSCs.

Conclusions

Equine SF may be a novel source of multipotent MSCs that have the ability to regenerate chondrocytes. Since collecting SF is less invasive than collecting BM or AT, SF-MSCs could be used to develop a practical strategy for cartilage regeneration following arthroscopic surgery in horses.

Conflict of interest statement

None of the authors has any financial or personal relationships that could inappropriately influence or bias the content of the paper.

Acknowledgements

The authors acknowledge Dr Douglas Antczak, Mr Donald Miller and Ms Becky Harman for the gifts of the antibodies against CD11a/18, and MHC classes I and II. This study was supported by Japan Society for the Promotion of Science (Grant number 25660242 to KM).

Appendix: Supplementary material

Supplementary data associated with this article can be found in the online version at doi:10.1016/j.tvjl.2014.07.029.

References

Arnhold, S.J., Goletz, I., Klein, H., Stumpf, G., Beluche, L.A., Rohde, C., Addicks, K., Litzke, L.F., 2007. Isolation and characterization of bone marrow-derived equine mesenchymal stem cells. American Journal of Veterinary Research 68, 1095–1105.

Barberini, D.J., Freitas, N.P., Magnoni, M.S., Maia, L., Listoni, A.J., Heckler, M.C., Sudano, M.J., Golim, M.A., Landim-Alvarenga, F.D., Amorim, R.M., 2014. Equine mesenchymal stem cells from bone marrow, adipose tissue and umbilical cord: Immunophenotypic characterization and differentiation potential. Stem Cell Research and Therapy 5, 25.

Braun, J., Hack, A., Weis-Klemm, M., Conrad, S., Treml, S., Kohler, K., Walliser, U., Skutella, T., Aicher, W.K., 2010. Evaluation of the osteogenic and chondrogenic differentiation capacities of equine adipose tissue-derived mesenchymal stem cells. American Journal of Veterinary Research 71, 1228–1236.

Burk, J., Ribitsch, I., Gittel, C., Juelke, H., Kasper, C., Staszyk, C., Brehm, W., 2013. Growth and differentiation characteristics of equine mesenchymal stromal cells derived from different sources. The Veterinary Journal 195, 98–106.

Friedenstein, A.J., 1976. Precursor cells of mechanocytes. International Review of Cytology 47, 327–359.

Jones, E.A., English, A., Henshaw, K., Kinsey, S.E., Markham, A.F., Emery, P., McGonagle, D., 2004. Enumeration and phenotypic characterization of synovial fluid multipotential mesenchymal progenitor cells in inflammatory and degenerative arthritis. Arthritis and Rheumatism 50, 817–827.

Kearns, C.F., McKeever, K.H., Malinowski, K., Struck, M.B., Abe, T., 2001. Chronic administration of therapeutic levels of clenbuterol acts as a repartitioning agent. Journal of Applied Physiology 91, 2064–2070.

Lee, J.I., Sato, M., Kim, H.W., Mochida, J., 2011. Transplantation of scaffold-free spheroids composed of synovium-derived cells and chondrocytes for the treatment of cartilage defects of the knee. European Cells and Materials 22, 275–290.

Mohanty, N., Gulati, B.R., Kumar, R., Gera, S., Kumar, P., Somasundaram, R.K., Kumar, S., 2014. Immunophenotypic characterization and tenogenic differentiation of mesenchymal stromal cells isolated from equine umbilical cord blood. In Vitro Cellular and Developmental Biology. Animal 50, 538–548.

Morito, T., Muneta, T., Hara, K., Ju, Y.J., Mochizuki, T., Makino, H., Umezawa, A., Sekiya, I., 2008. Synovial fluid-derived mesenchymal stem cells increase after intra-articular ligament injury in humans. Rheumatology 47, 1137–1143.

Nimura, A., Muneta, T., Koga, H., Mochizuki, T., Suzuki, K., Makino, H., Umezawa, A., Sekiya, I., 2008. Increased proliferation of human synovial mesenchymal stem cells with autologous human serum: Comparisons with bone marrow mesenchymal stem cells and with fetal bovine serum. Arthritis and Rheumatism 58, 501–510.

Sakaguchi, Y., Sekiya, I., Yagishita, K., Muneta, T., 2005. Comparison of human stem cells derived from various mesenchymal tissues: Superiority of synovium as a cell source. Arthritis and Rheumatism 52, 2521–2529.

Sekiya, I., Ojima, M., Suzuki, S., Yamaga, M., Horie, M., Koga, H., Tsuji, K., Miyaguchi, K., Ogishima, S., Tanaka, H., et al., 2012. Human mesenchymal stem cells in synovial fluid increase in the knee with degenerated cartilage and osteoarthritis. Journal of Orthopaedic Research 30, 943–949.

Suzuki, S., Muneta, T., Tsuji, K., Ichinose, S., Makino, H., Umezawa, A., Sekiya, I., 2012. Properties and usefulness of aggregates of synovial mesenchymal stem cells as a source for cartilage regeneration. Arthritis Research and Therapy 14, R136.

Vidal, M.A., Kilroy, G.E., Lopez, M.J., Johnson, J.R., Moore, R.M., Gimble, J.M., 2007. Characterization of equine adipose tissue-derived stromal cells: Adipogenic and osteogenic capacity and comparison with bone marrow-derived mesenchymal stromal cells. Veterinary Surgery 36, 613–622.